EUROPEAN ORGANIZATION FOR NUCLEAR RESEARCH

CERN-PPE/96-51
12th April 1996
(Revised 19th August 1996)

A study of charm hadron production in $Z^0 \to c\bar{c}$ and $Z^0 \to b\bar{b}$ decays at LEP

The OPAL Collaboration

Abstract

Measurements of the production of the weakly decaying charmed hadrons: D^0, D^+, D_s^+ and Λ_c^+ in both $Z^0 \to c\bar{c}$ and $Z^0 \to b\bar{b}$ events are reported. By summing the partial contributions from each of these states we measure the partial width for Z^0 decays into a $c\bar{c}$ pair as:

$$\frac{\Gamma_{c\bar{c}}}{\Gamma_{had}} = 0.167 \pm 0.011(stat) \pm 0.011(sys) \pm 0.005(br)$$

where the errors are statistical, systematic and due to the uncertainties in the charmed hadron branching ratios, respectively. The relative production rates for the formation of the charmed hadrons from primary c quarks is found to be in good agreement with continuum e^+e^- data at $\sqrt{s} \approx 10$ GeV.

The measured rates of these four charmed hadrons in b hadron decays is found to account for

$$1.061 \pm 0.045(stat) \pm 0.060(sys) \pm 0.037(br)$$

c or $\bar{c}$ quarks per b hadron decay. Comparison of the relative rates of the different charmed hadron species with $\Upsilon(4S)$ data indicates higher rates for D_s^+ and Λ_c^+ hadrons and lower rates of D^0 and D^+ mesons as expected due to the different mixture of b hadrons.

(Submitted to Z. Phys.)

The OPAL Collaboration

G. Alexander[23], J. Allison[16], N. Altekamp[5], K. Ametewee[25], K.J. Anderson[9], S. Anderson[12], S. Arcelli[2], S. Asai[24], D. Axen[29], G. Azuelos[18,a], A.H. Ball[17], E. Barberio[26], R.J. Barlow[16], R. Bartoldus[3], J.R. Batley[5], G. Beaudoin[18], J. Bechtluft[14], C. Beeston[16], T. Behnke[8], A.N. Bell[1], K.W. Bell[20], G. Bella[23], S. Bentvelsen[8], P. Berlich[10], S. Bethke[14], O. Biebel[14], V. Blobel[8], I.J. Bloodworth[1], J.E. Bloomer[1], P. Bock[11], H.M. Bosch[11], M. Boutemeur[18], B.T. Bouwens[12], S. Braibant[12], R.M. Brown[20], H.J. Burckhart[8], C. Burgard[27], R. Bürgin[10], P. Capiluppi[2], R.K. Carnegie[6], A.A. Carter[13], J.R. Carter[5], C.Y. Chang[17], C. Charlesworth[6], D.G. Charlton[1,b], D. Chrisman[4], S.L. Chu[4], P.E.L. Clarke[15], I. Cohen[23], J.E. Conboy[15], O.C. Cooke[16], M. Cuffiani[2], S. Dado[22], C. Dallapiccola[17], G.M. Dallavalle[2], S. De Jong[12], L.A. del Pozo[8], K. Desch[3], M.S. Dixit[7], E. do Couto e Silva[12], M. Doucet[18], E. Duchovni[26], G. Duckeck[8], I.P. Duerdoth[16], J.E.G. Edwards[16], P.G. Estabrooks[6], H.G. Evans[9], M. Evans[13], F. Fabbri[2], P. Fath[11], F. Fiedler[12], M. Fierro[2], H.M. Fischer[3], R. Folman[26], D.G. Fong[17], M. Foucher[17], H. Fukui[24], A. Fürtjes[8], P. Gagnon[7], A. Gaidot[21], J.W. Gary[4], J. Gascon[18], S.M. Gascon-Shotkin[17], N.I. Geddes[20], C. Geich-Gimbel[3], F.X. Gentit[21], T. Geralis[20], G. Giacomelli[2], P. Giacomelli[4], R. Giacomelli[2], V. Gibson[5], W.R. Gibson[13], D.M. Gingrich[30,a], J. Goldberg[22], M.J. Goodrick[5], W. Gorn[4], C. Grandi[2], E. Gross[26], M. Gruwé[8], C. Hajdu[32], G.G. Hanson[12], M. Hansroul[8], M. Hapke[13], C.K. Hargrove[7], P.A. Hart[9], C. Hartmann[3], M. Hauschild[8], C.M. Hawkes[5], R. Hawkings[8], R.J. Hemingway[6], G. Herten[10], R.D. Heuer[8], M.D. Hildreth[8], J.C. Hill[5], S.J. Hillier[1], T. Hilse[10], J. Hoare[5], P.R. Hobson[25], R.J. Homer[1], A.K. Honma[28,a], D. Horváth[32,c], R. Howard[29], R.E. Hughes-Jones[16], D.E. Hutchcroft[5], P. Igo-Kemenes[11], D.C. Imrie[25], M.R. Ingram[16], A. Jawahery[17], P.W. Jeffreys[20], H. Jeremie[18], M. Jimack[1], A. Joly[18], C.R. Jones[5], G. Jones[16], M. Jones[6], R.W.L. Jones[8], U. Jost[11], P. Jovanovic[1], T.R. Junk[8], D. Karlen[6], K. Kawagoe[24], T. Kawamoto[24], R.K. Keeler[28], R.G. Kellogg[17], B.W. Kennedy[20], B.J. King[8], J. Kirk[29], S. Kluth[8], T. Kobayashi[24], M. Kobel[10], D.S. Koetke[6], T.P. Kokott[3], S. Komamiya[24], R. Kowalewski[8], T. Kress[11], P. Krieger[6], J. von Krogh[11], P. Kyberd[13], G.D. Lafferty[16], H. Lafoux[21], R. Lahmann[17], W.P. Lai[19], D. Lanske[14], J. Lauber[15], S.R. Lautenschlager[31], J.G. Layter[4], D. Lazic[22], A.M. Lee[31], E. Lefebvre[18], D. Lellouch[26], J. Letts[2], L. Levinson[26], C. Lewis[15], S.L. Lloyd[13], F.K. Loebinger[16], G.D. Long[17], M.J. Losty[7], J. Ludwig[10], A. Luig[10], A. Malik[21], M. Mannelli[8], S. Marcellini[2], C. Markus[3], A.J. Martin[13], J.P. Martin[18], G. Martinez[17], T. Mashimo[24], W. Matthews[25], P. Mättig[3], W.J. McDonald[30], J. McKenna[29], E.A. Mckigney[15], T.J. McMahon[1], A.I. McNab[13], R.A. McPherson[8], F. Meijers[8], S. Menke[3], F.S. Merritt[9], H. Mes[7], J. Meyer[27], A. Michelini[2], G. Mikenberg[26], D.J. Miller[15], R. Mir[26], W. Mohr[10], A. Montanari[2], T. Mori[24], M. Morii[24], U. Müller[3], H.A. Neal[8], B. Nellen[3], B. Nijjhar[16], R. Nisius[8], S.W. O'Neale[1], F.G. Oakham[7], F. Odorici[2], H.O. Ogren[12], T. Omori[24], M.J. Oreglia[9], S. Orito[24], J. Pálinkás[33,d], J.P. Pansart[21], G. Pásztor[32], J.R. Pater[16], G.N. Patrick[20], M.J. Pearce[1], S. Petzold[27], P. Pfeifenschneider[14], J.E. Pilcher[9], J. Pinfold[30], D.E. Plane[8], P. Poffenberger[28], B. Poli[2], A. Posthaus[3], H. Przysiezniak[30], D.L. Rees[1], D. Rigby[1], S.A. Robins[13], N. Rodning[30], J.M. Roney[28], A. Rooke[15], E. Ros[8], A.M. Rossi[2], M. Rosvick[28], P. Routenburg[30], Y. Rozen[8], K. Runge[10], O. Runolfsson[8], U. Ruppel[14], D.R. Rust[12], R. Rylko[25], E.K.G. Sarkisyan[23], M. Sasaki[24], C. Sbarra[2], A.D. Schaile[8,e], O. Schaile[10], F. Scharf[3], P. Scharff-Hansen[8], P. Schenk[4], B. Schmitt[3], S. Schmitt[11], M. Schröder[8], H.C. Schultz-Coulon[10], M. Schulz[8], P. Schütz[3], W.G. Scott[20], T.G. Shears[16], B.C. Shen[4], C.H. Shepherd-Themistocleous[27], P. Sherwood[15], G.P. Siroli[2], A. Sittler[27], A. Skillman[15], A. Skuja[17], A.M. Smith[8], T.J. Smith[28], G.A. Snow[17], R. Sobie[28], S. Söldner-Rembold[10], R.W. Springer[30], M. Sproston[20], A. Stahl[3], M. Starks[12], M. Steiert[11], K. Stephens[16], J. Steuerer[27], B. Stockhausen[3], D. Strom[19], F. Strumia[8], P. Szymanski[20], R. Tafirout[18], S.D. Talbot[1], S. Tanaka[24], P. Taras[18], S. Tarem[22], M. Tecchio[8], M. Thiergen[10], M.A. Thomson[8], E. von Törne[3], S. Towers[6], M. Tscheulin[10], T. Tsukamoto[24], E. Tsur[23], A.S. Turcot[9], M.F. Turner-Watson[8], P. Utzat[11], R. Van Kooten[12], G. Vasseur[21], M. Verzocchi[10], P. Vikas[18], M. Vincter[28], E.H. Vokurka[16], F. Wäckerle[10], A. Wagner[27], C.P. Ward[5], D.R. Ward[5],

J.J. Ward[15], P.M. Watkins[1], A.T. Watson[1], N.K. Watson[7], P. Weber[6], P.S. Wells[8], N. Wermes[3], J.S. White[28], B. Wilkens[10], G.W. Wilson[27], J.A. Wilson[1], T. Wlodek[26], G. Wolf[26], S. Wotton[5], T.R. Wyatt[16], S. Yamashita[24], G. Yekutieli[26], V. Zacek[18],

[1]School of Physics and Space Research, University of Birmingham, Birmingham B15 2TT, UK
[2]Dipartimento di Fisica dell' Università di Bologna and INFN, I-40126 Bologna, Italy
[3]Physikalisches Institut, Universität Bonn, D-53115 Bonn, Germany
[4]Department of Physics, University of California, Riverside CA 92521, USA
[5]Cavendish Laboratory, Cambridge CB3 0HE, UK
[6] Ottawa-Carleton Institute for Physics, Department of Physics, Carleton University, Ottawa, Ontario K1S 5B6, Canada
[7]Centre for Research in Particle Physics, Carleton University, Ottawa, Ontario K1S 5B6, Canada
[8]CERN, European Organisation for Particle Physics, CH-1211 Geneva 23, Switzerland
[9]Enrico Fermi Institute and Department of Physics, University of Chicago, Chicago IL 60637, USA
[10]Fakultät für Physik, Albert Ludwigs Universität, D-79104 Freiburg, Germany
[11]Physikalisches Institut, Universität Heidelberg, D-69120 Heidelberg, Germany
[12]Indiana University, Department of Physics, Swain Hall West 117, Bloomington IN 47405, USA
[13]Queen Mary and Westfield College, University of London, London E1 4NS, UK
[14]Technische Hochschule Aachen, III Physikalisches Institut, Sommerfeldstrasse 26-28, D-52056 Aachen, Germany
[15]University College London, London WC1E 6BT, UK
[16]Department of Physics, Schuster Laboratory, The University, Manchester M13 9PL, UK
[17]Department of Physics, University of Maryland, College Park, MD 20742, USA
[18]Laboratoire de Physique Nucléaire, Université de Montréal, Montréal, Quebec H3C 3J7, Canada
[19]University of Oregon, Department of Physics, Eugene OR 97403, USA
[20]Rutherford Appleton Laboratory, Chilton, Didcot, Oxfordshire OX11 0QX, UK
[21]CEA, DAPNIA/SPP, CE-Saclay, F-91191 Gif-sur-Yvette, France
[22]Department of Physics, Technion-Israel Institute of Technology, Haifa 32000, Israel
[23]Department of Physics and Astronomy, Tel Aviv University, Tel Aviv 69978, Israel
[24]International Centre for Elementary Particle Physics and Department of Physics, University of Tokyo, Tokyo 113, and Kobe University, Kobe 657, Japan
[25]Brunel University, Uxbridge, Middlesex UB8 3PH, UK
[26]Particle Physics Department, Weizmann Institute of Science, Rehovot 76100, Israel
[27]Universität Hamburg/DESY, II Institut für Experimental Physik, Notkestrasse 85, D-22607 Hamburg, Germany
[28]University of Victoria, Department of Physics, P O Box 3055, Victoria BC V8W 3P6, Canada
[29]University of British Columbia, Department of Physics, Vancouver BC V6T 1Z1, Canada
[30]University of Alberta, Department of Physics, Edmonton AB T6G 2J1, Canada
[31]Duke University, Dept of Physics, Durham, NC 27708-0305, USA
[32]Research Institute for Particle and Nuclear Physics, H-1525 Budapest, P O Box 49, Hungary
[33]Institute of Nuclear Research, H-4001 Debrecen, P O Box 51, Hungary

[a] and at TRIUMF, Vancouver, Canada V6T 2A3
[b] and Royal Society University Research Fellow
[c] and Institute of Nuclear Research, Debrecen, Hungary
[d] and Department of Experimental Physics, Lajos Kossuth University, Debrecen, Hungary
[e] and Ludwig-Maximilians-Universität, München, Germany

1 Introduction

Charmed hadrons are known to be copiously produced in both $Z^0 \to c\bar{c}$ and $Z^0 \to b\bar{b}$ decays. Although the production of the different charmed hadrons has been studied in detail in continuum e^+e^- annihilations at $\sqrt{s} \approx 10$ GeV [1, 2, 3] and in the decays of B mesons produced in $\Upsilon(4S)$ decays [2, 4, 5], no comprehensive studies have been carried out at higher energies.

In this paper we present measurements of the production rates for the four dominant weakly decaying charmed hadrons: D^0, D^+, D_s^+ and Λ_c^+. Since more than 98% of primary charm quarks and most b hadron decays are expected to result in these states, the combination of these results allows one to obtain a comprehensive picture of charm production. The charmed hadrons are reconstructed in the decay modes[1]:

$$\begin{aligned} &D^0 \to K^-\pi^+, && D^+ \to K^-\pi^+\pi^+, \\ &D_s^+ \to \phi(1020)\pi^+, && D_s^+ \to \overline{K}^*(892)^0K^+, \\ &\Lambda_c^+ \to pK^-\pi^+. \end{aligned}$$

In order to separate primary charm production in $Z^0 \to c\bar{c}$ events from charm hadrons produced in b hadron decays, the apparent decay length distributions and energy spectra of the charmed hadrons are utilized. Because of the relatively large b hadron lifetimes and hard b fragmentation, charmed hadrons originating from b hadron decays have significantly longer apparent decay lengths than those from primary production. In addition the energy spectrum of these charmed hadrons is much softer than that due to primary charm production.

The measurements of charm hadron production from primary c quarks may be used to measure $\Gamma_{c\bar{c}}/\Gamma_{had}$. In the method presented in this paper $\Gamma_{c\bar{c}}/\Gamma_{had}$ is determined by summing the partial contributions from each of the four charmed hadrons, correcting for the small additional contribution expected from strange-charmed baryons.

Theoretical expectations for the charm multiplicity, n_c, in b hadron decays are typically in the range 1.11–1.30 [6, 7]. The measurement of n_c is of particular interest because the value inferred from the ARGUS [2, 4] and CLEO [5] data is at the lower end of the theoretical expectations. Since the mixture of b hadrons and the experimental systematics are different at LEP, it is important to make an independent measurement of this quantity. By comparing LEP measurements with $\Upsilon(4S)$ data one may also expect to learn about the production rates and decay modes of the B_s^0 and b baryons.

2 The OPAL detector

A complete description of the OPAL detector may be found elsewhere [8]. We describe briefly the aspects of the detector pertinent to this analysis. Charged particle tracking is performed by the central detector which consists of a large volume jet chamber, a precision vertex drift chamber and chambers measuring the z-coordinate[2] of tracks as they leave the jet chamber. In 1991 this tracking system was enhanced by the addition of a silicon microvertex detector providing $r-\phi$ coordinate measurements. For the 1993 run this device was replaced by an improved detector providing additional z coordinate measurements, but only the $r-\phi$

[1] Charge conjugation is implicitly implied throughout this paper.

[2] The OPAL coordinate system is defined with positive z being along the electron beam direction, θ and ϕ being the polar and azimuthal angles respectively.

information is used in this analysis. The $r-\phi$ tracking precision provided by both silicon detectors is almost identical, with space-point resolutions, including alignment uncertainties, of about 9 μm. When combined with the angle and curvature information provided by the other central detector components this results in an impact parameter resolution of 15 μm for tracks in $Z^0 \to \mu^+\mu^-$ and $Z^0 \to e^+e^-$ events. The central detector is positioned inside a solenoidal coil that provides a uniform magnetic field of 0.435 T. The momentum resolution obtained is approximately $(\sigma_{p_{xy}}/p_{xy})^2 = (0.02)^2 + (0.0015 p_{xy})^2$, where p_{xy} is the momentum transverse to the beam direction in GeV. In addition to tracking charged particles, the jet chamber provides measurements of the ionization loss, $\mathrm{d}E/\mathrm{d}x$, of charged particles, which are used for particle identification [9]. For the momentum region between 2 GeV and 20 GeV the separation between pions and kaons is greater than two standard deviations. The coil is surrounded by a time-of-flight counter array and a lead-glass electromagnetic calorimeter with presampler. Outside the electromagnetic calorimeter is the instrumented return yoke of the magnet, which forms the hadron calorimeter. This is surrounded by muon chambers.

3 Event selection

This analysis uses all OPAL data recorded in 1992 and 1993, as well as those collected after the silicon microvertex detector was commissioned in 1991. The data consist of e^+e^- annihilations at centre of mass energies between 88.5 and 93.8 GeV. The selection criteria for hadronic Z^0 decays are described elsewhere[10] and have an efficiency of $(98.4 \pm 0.4)\%$. After data quality and detector performance requirements, the available data sample consists of 1.71 million events.

Candidates for the decays $D^0 \to K^-\pi^+$, $D^+ \to K^-\pi^+\pi^+$, $D_s^+ \to \phi\pi^+, \phi \to K^+K^-$, $D_s^+ \to \overline{K}^{*0}K^+, \overline{K}^{*0} \to K^-\pi^+$ and $\Lambda_c^+ \to pK^-\pi^+$ are formed by considering all possible combinations of pion, kaon and proton track candidates. Pion, kaon and proton track candidates are selected using $\mathrm{d}E/\mathrm{d}x$ information from the jet chamber. Pion candidates are required to have a momentum greater than 0.5 GeV, whilst kaon and proton candidates are required to have a momentum greater than 2 GeV. All particle candidates are required to have a $\mathrm{d}E/\mathrm{d}x$ measurement [9] consistent with the hypothesized particle type with a corresponding probability greater than 1%. In addition, for kaons and protons, if the measured $\mathrm{d}E/\mathrm{d}x$ is larger than the expected value, we tighten this requirement to be greater than 3%. This requirement suppresses pion background because, in the momentum range of interest, pions have a larger expected $\mathrm{d}E/\mathrm{d}x$ measurement than kaons. To suppress pion background further, it is required that the kaon candidates in the decays $D^0 \to K^-\pi^+$, $D^+ \to K^-\pi^+\pi^+$ and $D_s^+ \to \overline{K}^{*0}K^+$ and at least one of the kaons in the mode $D_s^+ \to \phi\pi^+$ have a probability for a pion hypothesis less than 10%. Since the decay $\Lambda_c^+ \to pK^-\pi^+$ suffers from a relatively high level of combinatorial background, stronger particle identification criteria were applied. In this case, both proton and kaon candidates were required to have a probability for a pion hypothesis less than 1%.

All the charm hadron candidates were required to satisfy $|\cos\theta| < 0.85$ and to have $x_E = E_{X_c}/E_{beam} > 0.15$, where X_c indicates any of the charmed hadrons and E_{beam} is the beam energy.

In order to reject both fully and partially reconstructed $D^{*+} \to D^0\pi^+, D^0 \to K^-\pi^+X$ decays from the D^+ sample we require that the invariant masses of both $(K^-\pi^+)\pi^+$ combinations satisfy $m(K\pi\pi) - m(K\pi) > 0.16$ GeV.

For the two $D_s^+ \to K^+K^-\pi^+$ decays studied, the resonance substructure allows a significant

improvement in the signal to noise. $D_s^+ \to \phi\pi^+$ candidates were required to have a K^+K^- invariant mass in the range $1005 - 1035$ MeV and $D_s^+ \to \overline{K}^{*0}K^+$ candidates were required to have a $K^-\pi^+$ invariant mass in the range $845 - 945$ MeV. In addition to these requirements on the mass of the vector meson candidates, selection criteria were applied to the angle (θ_v) between the final state pseudoscalar meson (K or π) from the decay of the vector meson (ϕ or $\overline{K}^{*0}$), and the D_s^+, in the rest frame of the vector meson. This angle is distributed in proportion to $\cos^2\theta_v$ for true D_s^+ decays, but is close to flat for the combinatorial background. It was therefore required that $|\cos\theta_v| > 0.4(0.6)$ for the $D_s^+ \to \phi\pi^+(\overline{K}^{*0}K^+)$ decays respectively.

$D_s^+ \to \phi\pi^+$ decays are a potential background to the $\Lambda_c^+ \to pK^-\pi^+$ sample since the K^+ may be misidentified as a p. These are effectively removed by rejecting events where the invariant mass of the candidate pK^- combination, assuming a K^+K^- hypothesis, is in the range 1010-1030 MeV.

In order to reject decays having poor resolution and possibly bad reconstruction, we require that at least two of the charmed hadron decay tracks each be associated with at least one hit in the microvertex detector. This ensures precise vertex reconstruction. The χ^2 for the association of microvertex hits to tracks found in the other central tracking components is required to have a probability greater than 0.1%.

The charm hadron decay vertices are reconstructed in the r-ϕ plane. The apparent decay length is calculated in the r-ϕ plane using the position of the reconstructed vertex and the average e^+e^- interaction point. The average interaction point was determined using charged tracks from many consecutive events during that LEP fill. The decay length is signed according to the cosine of the angle between the charmed hadron momentum vector and the vector separating the decay vertex from the average interaction point. The decay length is converted into three dimensions using the charmed hadron direction cosines. For the three-track decays, where the vertex fit constraint has one degree of freedom, the χ^2 is required to be less than 15.

Use of the decay length information provides a powerful method of rejecting combinatorial background. To achieve significant background reduction the D^0, D_s^+ and Λ_c^+ candidates are required to have a decay length of more than 500 μm, whilst for the D^+ decay, candidates are required to have a decay length of at least 800 μm. Compared with the typical decay length resolutions, these requirements represent a decay length significance of approximately 1.5 and 2.0 standard deviations respectively.

The resulting invariant mass distributions are shown in figure 1. Clear signals are observed for each of the charmed hadrons.

4 Monte Carlo modelling

Simulated event samples were used to determine the reconstruction efficiencies and to study the sensitivity of the results to uncertainties in the physics processes responsible for charmed hadron production. These studies were carried out using the JETSET Monte Carlo program [12]. The parameters used in this model have been tuned to optimize the description of OPAL data [13]. The main features relevant to this analysis are modifications to the B hadron decay tables to describe better all available data [14], and allowing $L = 1$ P-wave mesons to be formed in both the fragmentation process and particle decays. Based on available LEP data on heavy flavour production [15, 16] the probability for forming a P-wave meson during fragmentation of c and b quarks was taken as 36%. The remaining 64% is accounted

for by vector and pseudoscalar mesons in the ratio 2.6:1. The B hadron lifetimes used were based on PDG averages [14] updated with more recently published results [17] which give: $\tau(\mathrm{B}^+) = 1.64 \pm 0.07$ ps, $\tau(\mathrm{B}^0) = 1.57 \pm 0.08$ ps, $\tau(\mathrm{B}_s^0) = 1.55 \pm 0.12$ ps and an average b baryon lifetime of 1.12 ± 0.08 ps. The b hadrons were fragmented according to the model of Peterson *et al.* [11]. Within the framework of this tune, which has [3] $\Lambda_{\mathrm{LLA}} = 250$ MeV [12], we are able to match our results [18] of $\langle x_E \rangle = 0.695$ for $\mathrm{B}^0/\mathrm{B}^+$ mesons, with a Peterson fragmentation parameter, $\epsilon_b = 0.0038$.

To simulate the detector response, event samples were processed using a detailed simulation of the OPAL detector [19]. This simulation has been tuned to describe the impact parameter, angular and curvature resolutions measured in OPAL data. After this tuning good agreement is found between the vertex and mass resolutions measured in data and the simulations. Uncertainties in the tracking resolutions are treated as systematic errors.

In order to determine the reconstruction efficiencies samples of JETSET simulated events were generated for each of the exclusive decays in both $\mathrm{Z}^0 \to c\bar{c}$ and $\mathrm{Z}^0 \to b\bar{b}$ events. In each case the number of events in the simulated samples was at least 2.5 times larger than the number of events expected in the data. For these simulated samples the overall efficiencies including the $x_E > 0.15$ requirement are listed in table 1. The efficiencies for the two D_s^+ decay

Decay Mode	$\eta(c \to \mathrm{X}_c)$ (%)	$\eta(b \to \mathrm{X}_b)$ (%)
$\mathrm{D}^0 \to \mathrm{K}^-\pi^+$	20.1 ± 0.2	23.9 ± 0.2
$\mathrm{D}^+ \to \mathrm{K}^-\pi^+\pi^+$	20.0 ± 0.2	21.0 ± 0.2
$\mathrm{D}_s^+ \to \phi\pi^+$	15.7 ± 0.3	18.9 ± 0.3
$\mathrm{D}_s^+ \to \overline{\mathrm{K}}^{*0}\mathrm{K}^+$	6.7 ± 0.2	8.1 ± 0.2
$\Lambda_c^+ \to \mathrm{pK}^-\pi^+$	6.3 ± 0.2	10.6 ± 0.3

Table 1: Reconstruction efficiencies for the charmed hadrons produced from primary charm quarks $\eta(c \to \mathrm{X}_c)$ and in b hadron decays $\eta(b \to \mathrm{X}_b)$.

channels include the ϕ and $\overline{\mathrm{K}}^{*0}$ branching ratios to the appropriate final state. The efficiencies are different for $c \to \mathrm{X}_c$ events compared with $b \to \mathrm{X}_c$ events because of the different energy spectra and decay length distributions. It should be noted that the efficiencies used in the remainder of this analysis are evaluated in bins of x_E and decay length, separately for prompt and b hadron decays.

5 Mass fits

By studying the simulations, it was found that the signals can not be well described by a single Gaussian resolution function. However, in each case it was found that a good description of the simulated data could be obtained by using a function consisting of the linear combination

[3] JETSET parameter PARJ(81).

Decay Mode	No. Events	Fitted Mass (MeV)	Narrow Gaussian σ (MeV)
$D^0 \to K^-\pi^+$	6461 ± 201	1863.8 ± 0.9	28.7 ± 0.9
$D^+ \to K^-\pi^+\pi^+$	5297 ± 269	1866.7 ± 1.2	23.1 ± 1.5
$D_s^+ \to \phi\pi^+$	638 ± 85	1967.3 ± 2.8	21.5 ± 3.0
$D_s^+ \to \overline{K}^{*0}K^+$	381 ± 86	1965.9 ± 4.7	24.3 ± 6.3
$\Lambda_c^+ \to pK^-\pi^+$	594 ± 101	2283.8 ± 4.0	22.1 ± 3.9

Table 2: Results of mass fits to the inclusive mass distribution.

of two Gaussians with a common mean. The mass resolutions vary as a function of x_E, but by allowing the width of the narrow Gaussian to vary, whilst keeping the fraction and relative width of the wider Gaussian fixed, a generally good description of the simulated signals was obtained. Typically it was found that using a wide Gaussian fraction of 10% and relative width of 6 provided the best description, but the fit results were insensitive to the precise values.

Using simulated samples, the different sources of backgrounds have also been investigated. In addition to the true combinatorial background, where the tracks are not associated with the decay of a single hadron, track combinations may result from partially reconstructed decays or be the result of particle misidentification. Due to kinematics, partially reconstructed charm decays form a significant fraction of the particle combinations in the mass regions below the charm signals. In particular, the $K^-\pi^+$ mass distribution shows a familiar satellite peak around 1.6 GeV, of width $\sim$ 70 MeV. This enhancement is largely the result of the decay $D^0 \to K^-\rho^+, \rho^+ \to \pi^+\pi^0$. Other partially reconstructed decay modes produce much less structure in the mass plots.

Particle misidentification may also result in structure in the mass distributions due to 'reflections' from other decay modes. In some cases these have been effectively eliminated during selection. For the $D^0 \to K^-\pi^+$ decay, there remains residual background close to the mass peak in the $K^-\pi^+$ mass distribution due to single particle misidentification in the decays $D^0 \to K^-K^+$, where the K^+ is misidentified as π^+ and double particle misidentification in the decay $\overline{D^0} \to \pi^-K^+$, where the kaon and pion assignments are reversed. These misidentification rates have been studied in the simulations and parameterized as a function of x_E. The simulation of the misidentification of $K^-\pi^+$ as π^-K^+ has been studied using a sample of $D^{*+} \to (K^-\pi^+)\pi^+$ decays and is found to be in good agreement with the data.

The D^+, D_s^+ and Λ_c^+ decays into three charged tracks may form 'reflections' in each other's mass distributions. These contributions were parameterized as a function of x_E and decay length using the simulations. Since *a priori* the relative rates of the different charmed hadrons were unknown, they were estimated assuming: $f(c \to D_s^+) = 12 \pm 4\%$, $f(b \to D_s^+) = 17 \pm 5\%$, $f(c \to \Lambda_c^+) = 8 \pm 4\%$ and $f(b \to \Lambda_c^+) = 11 \pm 3\%$. Here $f(c(b) \to X_c)$ is the probability that a primary $c(b)$ quark results in the production of a particular charmed hadron X_c or its

anti-particle[4]. It should be noted that these estimated rates are ultimately consistent with the results obtained in this analysis. The estimated errors were used for the evaluation of systematic uncertainties. With the exception of the $D_s^+ \to \phi\pi$ channel, the 'reflected' mass distributions are broad and do not produce significant distortions in the smooth background shapes.

The observed mass distributions were fitted using a binned maximum likelihood method to determine the number of signal events in the data. As a result of the Monte Carlo studies the fitted functions were chosen to consist of a linear combination of the signal Gaussians and polynomial functions, to describe the smoothly varying backgrounds. The polynomials were of fifth order for the D^0 and D^+ fits and third for the others. The contributions to the mass distributions from the 'reflection' backgrounds were also included. In the case of the $D^0 \to K^-\pi^+$ decay the contributions from $D^0 \to K^-K^+$ and misidentified $\overline{D^0} \to \pi^-K^+$ were fixed relative to the signal and the size of satellite was allowed to vary in the fit. For the other channels the absolute rates for the 'reflection' contribution were fixed to the predictions discussed above. For the $D_s^+ \to \phi\pi^+$ and $D_s^+ \to \overline{K}^{*0}K^+$ mass distributions it is expected that, in addition to the D_s signals, there may be contributions from fully reconstructed $D^+ \to \phi\pi^+$ and $D^+ \to \overline{K}^{*0}K^+$ decays, respectively. These were accounted for in the fits by allowing a second double Gaussian signal term.

The fitted signals are summarized in table 2 and illustrated in figure 1. In each case the fitted masses are in reasonable agreement with the PDG average [14] values.

6 Separation of charm and bottom decays

The lifetime information provided by the precise reconstruction of the charmed hadron decay vertices provides a means of separating the production mechanisms of the charmed hadrons. Because of the relatively large b hadron lifetimes and hard fragmentation the cascade charmed hadrons originating from b hadron decays have a distinctly different decay length distribution compared with prompt[5] production. The differences are more distinct for the D^0, D_s^+ and Λ_c^+ than the D^+ because of their shorter lifetimes. Neglecting experimental resolution, the decay length distributions for promptly produced charm hadrons in $Z^0 \to c\bar{c}$ decays of fixed energy are given by simple exponential distributions. Because the charm hadron lifetimes are precisely known, there is little systematic uncertainty in these distributions. In contrast the decay length distributions for cascade charmed hadrons are more complicated, being the convolution of the two exponential functions corresponding to the b hadron and charm decay distributions and the b hadron energy spectrum corresponding to a particular x_E. There are significant uncertainties in these distributions due to uncertainties in the b lifetimes, b fragmentation and the modelling of the b decays.

In order to utilize the decay length information to separate the different sources of charmed hadrons, the samples are subdivided into regions of x_E and decay length. Within each region a maximum likelihood fit to the mass spectrum is used to determine the number of signal events. The distribution of charm hadrons as a function of x_E and decay length is used as input to a χ^2 fit in order to separate the contributions from the two sources.

The D^0 and D^+ data distributions were each divided up into 13 regions of x_E, in steps

[4] $f(b \to X_c)$ has contributions from both the $b \to cX$ and and $b \to \bar{c}X$ processes.

[5] This includes charm hadrons produced in the fragmentation process as well as those resulting from primary c quarks.

of 0.05 between 0.15 and 0.70, 0.70–0.80 and greater than 0.80. Each x_E bin was subdivided into five decay length regions. Different decay length bins were chosen for the D^0 (0.05–0.15, 0.15–0.25, 0.25–0.35, 0.35–0.55 and 0.55–2.00 cm) and D^+ (0.08–0.25, 0.25–0.50, 0.50–0.75, 0.75–1.00 and 1.00–2.00 cm) to reflect the longer D^+ lifetime. Within each x_E bin the number of signal events was determined by a binned maximum likelihood fit simultaneously to the five decay length regions. These fits were similar to those used for the overall mass distributions described above, except the signal shape was constrained to be common between the five decay length regions with a common mean and narrow Gaussian width, which were allowed to vary in the fits. The background shape functions were allowed to vary independently. However, to reflect better the lower statistics, the orders of the polynomial backgrounds were reduced to three in the x_E regions below 0.55 (0.25) and two for higher x_E values for the D^0 (D^+). An example of one of the mass fits is shown in figure 2.

For the D_s^+ and Λ_c^+ decays, the lower statistics necessitate coarser binning. For these decays, four x_E bins (0.15–0.30, 0.30–0.45, 0.45–0.60 and 0.60–1.00) were used, each subdivided into three decay length regions (0.05–0.25, 0.25–0.45 and 0.45–2.00 cm). In order to improve the statistical precision of the mass fits to these samples the widths of the signal Gaussians were constrained to the predictions of the simulation. It should be noted that there is generally good agreement between the mass resolutions observed in the data and the simulation.

In all cases, the mass fits resulted in numbers of reconstructed charm hadrons as a function of x_E and decay length. Because of the simultaneous fitting technique, there are small correlations within each x_E region, which are taken into account by calculating the full covariance matrix. The total number of fitted events is in reasonable agreement with the simple fits to the overall mass distributions.

The observed distributions of charmed hadrons as a function of x_E region, i, and decay length region, j, were used to determine the number of charmed hadrons due to prompt (mainly from primary c quarks) production and b hadron decays. The expected number of events for each bin, n_{ji}^{pred}, may be expressed as follows:

$$n_{ji}^{pred} = N_i^p \sum_k (\eta_{jk}^p)_i (f_k^p)_i + N_i^b \sum_k (\eta_{jk}^b)_i (f_k^b)_i \tag{1}$$

where N_i^p (N_i^b) is the unknown total number of charmed hadrons due to prompt production (b hadron decays) in a particular x_E region i and f_i^p (f_i^b) is the true distribution of decay lengths normalized so that $\sum_k (f_k^p)_i = \sum_k (f_k^b)_i = 1$, where the summation is over true decay length regions, k. The $(\eta_{jk})_i$ are elements of efficiency matrices, which were determined using the exclusive fully simulated Monte Carlo samples. These allow for the mapping of the true decay length distributions onto the reconstructed distributions. Because the efficiencies depend on both the source of the charmed hadrons and uncertainties in the physics parameters used in the simulations, they were calculated separately for each x_E region i and decay length region j. The distributions of f_i^p and f_i^b may be taken from Monte Carlo samples without detector simulation. By varying these physics distributions the reconstruction efficiencies may be reweighted appropriately.

Using the efficiency matrices a χ^2 fit may be performed to the data in order to extract N_i^p and N_i^b:

$$\chi_i^2(N_i^p, N_i^b) = \vec{V}_i^T \sigma_i^{-1} \vec{V}_i \tag{2}$$

where $\vec{V}_i$ is a vector of fitted differences to the data, with elements $V_{ji} = n_{ji}^{data} - n_{ji}^{pred}$ and σ_i is the sum of the covariance matrices resulting from the mass fits and uncertainties in the

reconstruction efficiencies. It should be noted that in general N_i^p and N_i^b are anticorrelated. Therefore the uncertainty on the total rate, $N_i^p + N_i^b$, is typically much smaller than the quadrature sum of the two components.

7 Results for D^0 and D^+ production

The relatively high statistics available in the D^0 and D^+ samples allows a detailed study of the x_E distributions of D mesons produced in both the $c \to D$ and $b \to D$ processes. These samples have been used to study these processes in both the context of several fragmentation models and a model independent way.

The fragmentation models considered in this paper are those of Peterson *et al.* [11]

$$f(z) \propto z^{-1} \left(1 - \frac{1}{z} - \frac{\epsilon}{(1-z)}\right)^{-2},$$

Collins and Spiller [20]

$$f(z) \propto \left(\frac{(1-z)}{z} + \frac{(2-z)\tilde{\epsilon}}{(1-z)}\right)(1+z^2)\left(1 - \frac{1}{z} - \frac{\tilde{\epsilon}}{(1-z)}\right)^{-2},$$

Kartvelishvili [21]

$$f(z) \propto z^{\alpha}(1-z),$$

and the Lund Group [22]

$$f(z) \propto \frac{1}{z}(1-z)^a e^{(-\frac{bM_T^2}{z})}.$$

The first three of these models have one free parameter: $\epsilon, \tilde{\epsilon}$ and α respectively, while the Lund model has two parameters a and bM_T^2. Direct comparison of the data with these models is complicated because they are generally a function of the fragmentation variable, z, which is not directly observable and model dependent[6]. The mapping of the z distribution onto the observable x_E distribution requires a simulation to account for QCD effects. In addition this mapping is sensitive to features of the fragmentation process, for example, the fraction (f^{**}) of primary c quarks which fragment to P-wave or higher mass states. For these studies we used the OPAL tuned JETSET simulation as described in section 4.

The presence of a small fraction of D mesons formed during fragmentation, mainly via the gluon splitting process $g \to c\bar{c}$, presents an additional complication. The resulting D mesons have a very soft x_E distribution, with about 50% having $x_E < 0.15$. The decay length distribution does not allow us to separate this process from the primary D mesons. The first experimental evidence for this process has recently been reported by OPAL [23, 24]. The measured rate for this process is $(2.27 \pm 0.28 \pm 0.41) \times 10^{-2}$ per hadronic event, which corresponds to 1.4 ± 0.3 times the JETSET predictions, but, because of the limited statistics, this does not provide a constraint on the x_E distribution of D mesons originating from this process. Therefore, because we are relatively insensitive to prompt D production in the low

[6] We use the JETSET definition, $z = (E+p_{\parallel})_{hadron}/(E+p_{\parallel})_{available}$, where $p_{\parallel}$ is the momentum component in the quark direction.

Model	$p_{c\to \mathrm{D}^0}$ ($\times 10^{-3}$)	$p_{b\to \mathrm{D}^0}$ ($\times 10^{-3}$)	Total ($\times 10^{-2}$)	ε	$\langle x_E \rangle$	χ^2/df
Peterson	3.89 ± 0.27	4.54 ± 0.23	1.784 ± 0.066	0.027 ± 0.006	0.487 ± 0.009	58.5/50
Collins & Spiller	4.02 ± 0.28	4.49 ± 0.23	1.804 ± 0.066	0.037 ± 0.014	0.479 ± 0.010	58.1/50
Kartvelishvili	3.80 ± 0.28	4.55 ± 0.23	1.770 ± 0.066	4.96 ± 0.64	0.495 ± 0.011	60.0/50
Lund	3.93 ± 0.30	4.51 ± 0.23	1.786 ± 0.072	1.92 ± 0.32	0.487 ± 0.010	62.1/50
Model Indep.	4.11 ± 0.36	4.50 ± 0.26	1.824 ± 0.072	-	-	36.6/39

Model	$p_{c\to \mathrm{D}^+}$ ($\times 10^{-3}$)	$p_{b\to \mathrm{D}^+}$ ($\times 10^{-3}$)	Total ($\times 10^{-2}$)	ε	$\langle x_E \rangle$	χ^2/df
Peterson	3.58 ± 0.46	3.79 ± 0.31	1.548 ± 0.081	0.035 ± 0.012	0.483 ± 0.015	59.4/50
Collins & Spiller	3.66 ± 0.50	3.76 ± 0.31	1.560 ± 0.086	0.059 ± 0.032	0.473 ± 0.017	60.5/50
Kartvelishvili	3.49 ± 0.48	3.83 ± 0.31	1.540 ± 0.090	4.02 ± 0.78	0.484 ± 0.018	60.5/50
Lund	3.38 ± 0.47	3.91 ± 0.31	1.534 ± 0.093	1.55 ± 0.36	0.478 ± 0.018	61.0/50
Model Indep.	3.14 ± 0.55	4.08 ± 0.43	1.520 ± 0.086	-	-	45.8/39

Table 3: D meson production rates with different $c \to \mathrm{D}$ fragmentation models. The symbol ε is used to refer generically to the fitted fragmentation model parameters, and $\langle x_E \rangle_c$ is the average x_E value for D mesons formed from primary c quarks.

x_E region, we have chosen to fix the shapes of the x_E distributions to those predicted by JETSET, but to scale the rates by 1.4.

For each of the four fragmentation models we have fitted a model parameter and the overall normalization of the $c \to \mathrm{D}$ component. For the Lund model, the a parameter was fixed to be 0.18, as measured using inclusive event shapes [25] and an effective bM_T^2 was fitted. Because the x_E distribution of D mesons from b hadron decays is a complicated function of the b quark fragmentation and the b hadron decay modelling, which are not necessarily expected to be well modelled by the simulations, it is convenient to retain model independence by allowing the fitted number of $b \to \mathrm{D}$ events to vary freely within each x_E region. After constraining the functional forms of the prompt charm components, and summing over the χ_i^2 given by equation 2, the χ^2 function becomes:

$$\chi^2(N_{tot}^c, \varepsilon, N_{tot}^g, N_1^b, N_2^b, ...N_{13}^b) = \sum_i \vec{V}_i^T \sigma_i^{-1} \vec{V}_i, \tag{3}$$

where N_{tot}^c is the total number of $c \to \mathrm{D}$ events, ε is a fitted charm fragmentation model parameter, N_{tot}^g is the fixed total number of D mesons formed via the gluon splitting process $g \to c\bar{c}$ and the N_i^b are the number of D mesons from b hadron decays for each x_E region i.

Figure 3 shows the D^0 data and Peterson model fit results for two of the x_E regions. The different decay length distributions which allow the statistical separation of the prompt from the $b \to \mathrm{D}^0$ process are apparent.

Decay	$p_{c\to X_c}$ $(\times 10^{-3})$	$p_{b\to X_c}$ $(\times 10^{-3})$	Total $(\times 10^{-3})$	χ^2/df
$D_s^+ \to \phi\pi^+$	0.56 ± 0.15	1.66 ± 0.18	4.60 ± 0.36	23.6/19
$\Lambda_c^+ \to pK^-\pi^+$	0.41 ± 0.19	1.22 ± 0.23	3.45 ± 0.52	4.9/7

Table 4: Results of fits to the D_s^+ and Λ_c^+ data assuming Peterson fragmentation for the primary c components.

The results of the fits to the Peterson fragmentation model to the D^0 and D^+ data are shown in figure 4. The main figures show the fitted contribution from the $c \to D$ and $g \to D$ processes to the total measured rates, whilst the inserts compare the unfolded x_E spectra from $b \to D$ decays with those in the simulation. Reasonable agreement is observed.

A summary of the D^0 and D^+ fit results may be found in table 3. The results are expressed in terms of $p_{q\to D} = \Gamma_{q\bar{q}}/\Gamma_{had} \cdot f(q \to D) \cdot B_D$, where $\Gamma_{q\bar{q}}/\Gamma_{had}$ is the Z^0 partial width to a particular quark type q and B_D is the appropriate D branching ratio. In each case the quoted rates are corrected for efficiency and include the part of the x_E spectra below 0.15. For $b \to D$ decays the correction factors were obtained from the simulations and were found to be 1.15. The total rates are $2(p_{c\to D} + p_{b\to D})$ plus the estimated contribution from gluon splitting and correspond to $\bar{n}(Z^0 \to D) \cdot B_D$, the product of the D multiplicity in hadronic Z^0 decays and the appropriate D branching ratio. The errors are statistical only. It is apparent from the comparison of the χ^2 of the fits that we are currently unable to distinguish between the models. Therefore, in order to obtain our final results, we have chosen to use the results of the Peterson model fits and to use the other model fits to assess the systematic uncertainties.

As an additional cross-check we have also performed model independent fits to the data using equation 2 to fit each x_E region separately. These results are also included in table 3. To obtain the total primary charm production rates it is still necessary to make a small model dependent correction to correct for the region $x_E < 0.15$. This correction factor was estimated using the Peterson model to be 1.06. The results of these model independent fits were found to be consistent with the model dependent results.

8 Results for D_s^+ and Λ_c^+ production

Due to the lower statistics available in the D_s^+ and Λ_c^+ samples it is not possible to constrain significantly the charm fragmentation function. However, it is expected that the fragmentation model parameters which describe D_s^+ and Λ_c^+ production are similar to those for D^0 and D^+ mesons, since the first rank hadrons have similar masses. Therefore, in order to fit the D_s^+ and Λ_c^+ data we have used the results of the Peterson model fits to the D^0 and D^+ data. The average of the two channels gives $\epsilon_c = 0.029 \pm 0.005$. The uncertainty on this parameter and the results of the other fragmentation models were used to assess the systematic uncertainties.

After constraining the shape of the primary charm hadron spectra and fixing the rate expected from gluon splitting to be 1.4 times the JETSET prediction, the χ^2 fit analogous to equation 3 is reduced to a five parameter fit: N_{tot}^c and N_i^b for each of the four x_E regions. For the D_s^+ the two decay channels were combined into a single fit with the ratio fixed to the

PDG ratio of branching fractions [14]: $B(\mathrm{D}_s^+ \to \overline{\mathrm{K}}^{*0}\mathrm{K}^+)/B(\mathrm{D}_s^+ \to \phi\pi^+) = 0.95 \pm 0.10$. The results are expressed in terms of $B(\mathrm{D}_s^+ \to \phi\pi^+)$ and the uncertainty in this ratio is treated as a systematic error. The results of these χ^2 fits are summarized in table 4 and illustrated in figure 5. It may be seen that within the limited statistics the x_E distributions are similar to those observed for D^0 and D^+ mesons. However, for these states the overall fraction of events resulting from b hadron decays is larger than that found for D^0 and D^+ mesons. This is as generally expected, since D_s^+ and Λ_c^+ hadrons result from the decays of B^0 and B^+ mesons as well as forming the dominant charmed hadrons in B_s^0 and Λ_b^0 decays, respectively.

9 Systematic errors

The systematic errors in this analysis may be broadly divided into uncertainties in the physics assumed in the source separation fits and effects due to the modelling of the detector. We have considered the effect of each error on both the source separated measurements and the total $\mathrm{Z}^0 \to \mathrm{X}_c$ production rates. In addition we have investigated the sensitivity of the measurements of $\langle x_E \rangle$ for the D^0 and D^+ mesons to the different sources of systematic uncertainty. The results of these studies are summarized in tables 5, 6, 7 and 8.

The systematic errors due to uncertainties in the physics parameters assumed during the fits, *i.e.*, b hadron lifetimes, ϵ_b and the charmed hadron lifetimes have been evaluated by repeating the fits using physics distributions generated, in turn, with each of the parameters differing by its estimated uncertainty. The b hadron lifetimes were each varied independently by their uncertainties. The b hadron energy spectrum was varied by changing the Peterson fragmentation parameter in a range $0.0038^{+0.0016}_{-0.0010}$ corresponding to $\langle x_E \rangle$ of 0.695 ± 0.010[18]. The effects of different fragmentation models on the kinematic acceptance of the charmed hadrons in b decays has also been investigated by considering the four different fragmentation models used in reference [18]. These two errors have been combined in quadrature. The lifetimes of the charmed hadrons have also been varied by amounts corresponding to the errors on the PDG [14] averages. The source separated results are found to be fairly sensitive to the assumed b hadron lifetimes, but relatively insensitive to the other parameters.

In order to determine the total $b \to \mathrm{X}_c$ rates it is necessary to correct for the unobserved fraction with $x_E < 0.15$. Although the OPAL tuned simulation provides a good description of the x_E distribution in the region with $x_E > 0.15$, we have carried out a study of possible differences due to b hadron decay modelling. The size of these uncertainties was evaluated by considering the fraction of events with $x_E < 0.15$ for each of five categories of b hadron decays: semileptonic, two body $b \to \mathrm{X}_c\mathrm{X}$, two body $b \to \mathrm{X}_c\overline{\mathrm{X}}_c$, three body $b \to \mathrm{X}_c\mathrm{X}$, and $b \to \mathrm{X}_c\overline{\mathrm{X}}_c\mathrm{X}$, where X_c indicates a charmed hadron and X a non-charmed state. Although the types of decay result in different spectra there are only small differences in the fractions with $x_E < 0.15$. The largest deviations from the average were considered as the b decay model systematic errors.

Constraining the shape of the x_E distribution of D mesons to that predicted by the Peterson model clearly results in a systematic uncertainty. Because all of the models considered are able to give an adequate description of the data we have estimated the systematic uncertainty from the maximum variations of the model dependent fits from the Peterson results. These uncertainties are currently small compared with the statistical errors. With higher statistics it might be better to use the model independent method to reduce the total error. In the case of D_s^+ and Λ_c^+, the systematic errors have been estimated by using the average of the model fits

Systematic	D^0	D^+	D_s^+	Λ_c
$\tau(B^+) = 1.64 \pm 0.07$ ps	± 1.3 %	± 1.1 %	± 0.6 %	± 0.7 %
$\tau(B^0) = 1.57 \pm 0.08$ ps	± 1.1 %	± 2.5 %	± 1.0 %	± 1.0 %
$\tau(B_s^0) = 1.55 \pm 0.12$ ps	± 0.3 %	± 0.1 %	± 3.1 %	± 0.4 %
$\tau(b\,\text{baryon}) = 1.12 \pm 0.08$ ps	± 0.1 %	< 0.1 %	< 0.1 %	± 5.6 %
charm lifetimes	$^{+0.1}_{-0.3}$ %	$^{+0.4}_{-0.9}$ %	± 3.4 %	± 1.6 %
b fragmentation	± 0.7 %	± 0.8 %	$^{+1.5}_{-1.2}$ %	$^{+1.9}_{-6.4}$ %
c fragmentation model	$^{+3.4}_{-2.9}$ %	$^{+3.4}_{-5.4}$ %	$^{+7.5}_{-6.0}$ %	$^{+8.6}_{-7.6}$ %
$f_c^{**} = 36 \pm 18$ %	± 0.3 %	± 1.2 %	-	-
$\Gamma(g \to c\bar{c})$	± 0.8 %	± 0.6 %	± 0.3 %	± 0.4 %
$B(D_s^+ \to \overline{K}^{*0}K^+)/B(D_s^+ \to \phi\pi^+)$	-	-	± 0.5 %	-
dE/dx efficiency	± 3.1 %	± 3.1 %	± 6.4 %	± 4.7 %
Si Matching efficiency	± 1.5 %	± 0.5 %	± 0.5 %	± 0.5 %
Track resolution	$^{+1.6}_{-1.4}$ %	$^{+2.7}_{-2.5}$ %	± 3.1 %	± 7.1 %
Mass fits	$^{+2.9}_{-3.1}$ %	$^{+3.5}_{-3.5}$ %	± 5.3 %	± 9.4 %
Separation method	± 2.2 %	± 2.2 %	± 2.2 %	± 2.2 %
Total	$^{+6.6}_{-6.4}$ %	$^{+7.5}_{-8.6}$ %	$^{+12.8}_{-12.0}$ %	$^{+16.7}_{-17.3}$ %

Table 5: Relative systematic errors on $f(c \to D)$ measurements.

Systematic	D^0	D^+	D_s^+	Λ_c
$\tau(B^+) = 1.64 \pm 0.07$ ps	± 1.1 %	± 0.7 %	± 0.4 %	± 0.3 %
$\tau(B^0) = 1.57 \pm 0.08$ ps	± 0.9 %	± 2.2 %	± 0.6 %	± 0.4 %
$\tau(B_s^0) = 1.55 \pm 0.12$ ps	± 0.2 %	± 0.1 %	± 1.7 %	± 0.2 %
$\tau(b\,\text{baryon}) = 1.12 \pm 0.08$ ps	± 0.1 %	< 0.1 %	< 0.1 %	± 1.6 %
charm lifetimes	$^{-0.3}_{+0.4}$ %	$^{-1.0}_{+1.1}$ %	± 1.5 %	± 1.7 %
b fragmentation	$^{+1.5}_{-1.3}$ %	$^{+1.9}_{-1.8}$ %	± 1.4 %	± 1.8 %
b decay model	$^{+1.7}_{-0.7}$ %	$^{+1.7}_{-0.7}$ %	$^{+1.2}_{-1.0}$ %	± 1.0 %
c fragmentation model	$^{-1.0}_{+0.3}$ %	$^{+2.2}_{-0.6}$ %	$^{+1.0}_{-1.2}$ %	$^{+0.7}_{-1.0}$ %
$f_c^{**} = 36 \pm 18$ %	± 0.2 %	± 0.2 %	-	-
$\Gamma(g \to c\bar{c})$	± 0.3 %	± 0.4 %	± 0.3 %	± 0.2 %
$B(D_s^+ \to \overline{K}^{*0}K^+)/B(D_s^+ \to \phi\pi^+)$	-	-	± 1.3 %	-
dE/dx efficiency	± 3.1 %	± 3.1 %	± 6.4 %	± 4.7 %
Si Matching efficiency	± 1.5 %	± 0.5 %	± 0.5 %	± 0.5 %
Track resolution	$^{-1.4}_{+1.2}$ %	$^{-2.9}_{+2.7}$ %	± 1.6 %	± 1.6 %
Mass fits	$^{+2.9}_{-3.4}$ %	$^{+4.0}_{-3.3}$ %	± 6.0 %	± 5.5 %
Separation method	± 1.7 %	± 1.7 %	± 1.7 %	± 1.7 %
Total	$^{+5.7}_{-5.8}$ %	$^{+7.4}_{-6.5}$ %	± 9.7 %	± 8.2 %

Table 6: Relative systematic errors on $f(b \to D)$ measurements.

Systematic	D^0	D^+	D_s^+	Λ_c
$\tau(B^+) = 1.64 \pm 0.07$ ps	< 0.1 %	± 0.1 %	± 0.2 %	± 0.1 %
$\tau(B^0) = 1.57 \pm 0.08$ ps	< 0.1 %	± 0.2 %	± 0.2 %	± 0.1 %
$\tau(B_s^0) = 1.55 \pm 0.12$ ps	< 0.1 %	< 0.1 %	± 0.5 %	± 0.1 %
$\tau(b\,\text{baryon}) = 1.12 \pm 0.08$ ps	< 0.1 %	< 0.1 %	< 0.1 %	± 0.2 %
charm lifetimes	$^{+0.1}_{-0.3}$ %	$^{+0.4}_{-0.9}$ %	± 0.3 %	± 0.9 %
b fragmentation	± 0.7 %	± 1.0 %	± 0.8 %	± 0.2 %
b decay model	$^{+0.8}_{-0.4}$ %	$^{+0.8}_{-0.4}$ %	$^{+0.8}_{-0.7}$ %	$^{+0.8}_{-0.7}$ %
c fragmentation model	$^{+1.0}_{-0.3}$ %	$^{+0.7}_{-1.2}$ %	$^{+1.0}_{-0.7}$ %	$^{+1.5}_{-1.2}$ %
$f_c^{**} = 36 \pm 18$ %	± 0.2 %	± 0.2 %	-	-
$\Gamma(g \to c\bar{c})$	± 1.2 %	± 1.0 %	± 1.1 %	± 2.1 %
$B(D_s^+ \to \overline{K}^{*0}K^+)/B(D_s^+ \to \phi\pi^+)$	-	-	± 0.8 %	-
dE/dx efficiency	± 3.1 %	± 3.1 %	± 6.4 %	± 4.7 %
Si Matching efficiency	± 1.5 %	± 0.5 %	± 0.5 %	± 0.5 %
Track resolution	$^{+0.0}_{-0.1}$ %	$^{+1.1}_{-0.1}$ %	± 0.4 %	± 0.6 %
Mass fits	$^{+2.8}_{-2.9}$ %	$^{+3.8}_{-3.5}$ %	± 5.7 %	± 6.2 %
Total	± 4.8 %	$^{+5.3}_{-5.2}$ %	± 8.8 %	± 8.3 %

Table 7: Relative systematic errors on the inclusive charm production rate measurements.

Systematic	$\langle x_E(D^0)\rangle$	$\langle x_E(D^+)\rangle$
b lifetimes	$^{+0.003}_{-0.003}$	$^{+0.005}_{-0.004}$
b fragmentation	$^{+0.000}_{-0.004}$	$^{+0.001}_{-0.002}$
Charm lifetimes	± 0.001	$^{+0.000}_{-0.001}$
$f_c^{**} = 36 \pm 18\%$	$^{+0.005}_{-0.001}$	$^{+0.001}_{-0.002}$
$\Gamma(g \to c\bar{c})$	$^{+0.001}_{-0.000}$	± 0.001
Track resolution	$^{+0.005}_{-0.000}$	$^{+0.003}_{-0.002}$
Mass fits	$^{+0.003}_{-0.001}$	± 0.001
c fragmentation model	± 0.008	$^{+0.001}_{-0.010}$
Total	$^{+0.011}_{-0.009}$	$^{+0.007}_{-0.011}$

Table 8: Systematic errors on $\langle x_E \rangle$ measurements.

obtained from the D^0 and D^+ data and by varying the Peterson fit parameter by its statistical errors. These were combined in quadrature.

In order to evaluate the systematic errors due to uncertainties in f_c^{**} the fits were repeated using $z \to x_E$ mappings determined assuming $f_c^{**} = 0.18$ and $f_c^{**} = 0.54$. The observed changes were taken as systematic errors.

Uncertainties in the rate of the process $g \to c\bar{c}$ were taken into account by changing the rates by the uncertainty in the OPAL results [23, 24] and repeating the fits.

The reconstruction of the charmed mesons relies heavily on both the microvertex information and the particle identification provided by the $\mathrm{d}E/\mathrm{d}x$ measurements. It is therefore important to verify that both of these are well simulated by the Monte Carlo. Both of these requirements were studied using $D^{*+} \to (K^-\pi^+)\pi^+$ decays. A high purity sample of D^{*+} decays was obtained using requirements on the $m(K\pi\pi) - m(K\pi)$ mass difference, and on the reconstructed decay length. Using this sample the efficiencies of the $\mathrm{d}E/\mathrm{d}x$ requirements were studied and compared with the simulation, and good agreement was obtained. The relative statistical uncertainty on the efficiency corresponding to the selection criteria applied in the D^0 and D^+ analyses is 3.1%. Because the momentum spectrum of these decays closely matches the inclusive samples this uncertainty was considered a common overall systematic error.

A similar method was used to measure the efficiency of the proton $\mathrm{d}E/\mathrm{d}x$ selection using a sample of $\Lambda^0 \to p\pi^-$ decays. Again good agreement was obtained and the statistical uncertainty of the comparison has been included in the quoted $\mathrm{d}E/\mathrm{d}x$ systematic error quoted for $\Lambda_c^+ \to pK^-\pi^+$.

In addition, the special case of the kaons produced in $\phi \to K^+K^-$ in $D_s^+ \to \phi\pi^+$ was studied using a large inclusive sample of ϕ decays. The number of events in which both kaons passed the $\mathrm{d}E/\mathrm{d}x$ selection as a fraction of the events where at least one passed was found to be in good agreement with the detector simulation. The relative statistical uncertainty of this comparison was included in the $\mathrm{d}E/\mathrm{d}x$ systematic error quoted for $D_s^+ \to \phi\pi^+$.

The modelling of the association of silicon microvertex detector hits to tracks was studied in a similar way after requiring the D^{*+} sample to pass a tight $\mathrm{d}E/\mathrm{d}x$ selection. The efficiency for requiring both tracks to have silicon hits associated was found to be $82.0 \pm 1.5\%$ in the data and $82.2 \pm 0.6\%$ in the simulation. The relative statistical uncertainty (1.5%) was taken directly as the systematic error for the D^0 results. For the other decays the uncertainty is smaller because only two of the three tracks are required to be matched to silicon hits. In this case the systematic error was estimated assuming the matching of tracks is uncorrelated.

Uncertainties in the impact parameter and angular resolutions affect the vertex resolution. Because of the decay length requirements, this changes the overall efficiencies as well as the smearing between decay length bins. These uncertainties have been evaluated by repeating the analysis using efficiency matrices determined using Monte Carlo samples in which the track resolutions have been varied by $\pm 15\%$. The observed variations were treated as systematic errors.

Uncertainties in the mass resolutions have been studied by varying the fraction of events in the wide Gaussian by $\pm 25\%$. The observed variations were treated as systematic errors. It should be noted that there is good agreement been the mass resolutions observed in the data and the simulation. An additional source of systematic errors in the mass fits is the level of the misidentified backgrounds discussed in section 3. These errors were determined by changing the expected rates of the contributing processes by their uncertainties and repeating the analyses.

Finally we have conservatively assigned an error on the source separation fit method equal

to the statistical level to which it has been tested using high statistics samples generated using a fast simulation of the OPAL detector [19].

The total systematic errors were obtained by adding all of the components in quadrature.

10 Results

Our measurements of the production of D^0, D^+, D_s^+ and Λ_c^+ hadrons are summarized in table 9. The overall multiplicity measurements are equal to twice the sum of the contributions from primary c and b quarks plus the contributions from gluon splitting.

Particle	$\frac{\Gamma_{c\bar{c}}}{\Gamma_{had}} \cdot f(c \to \mathrm{X}_c) \cdot B_{\mathrm{X}_c}$ (%)	$\frac{\Gamma_{b\bar{b}}}{\Gamma_{had}} \cdot f(b \to \mathrm{X}_c) \cdot B_{\mathrm{X}_c}$ (%)	$\bar{n}(\mathrm{Z}^0 \to \mathrm{X}_c) \cdot B_{\mathrm{X}_c}$ (%)
D^0	$0.389 \pm 0.027^{+0.026}_{-0.024}$	$0.454 \pm 0.023^{+0.025}_{-0.026}$	$1.784 \pm 0.066 \pm 0.086$
D^+	$0.358 \pm 0.046^{+0.025}_{-0.031}$	$0.379 \pm 0.031^{+0.028}_{-0.025}$	$1.548 \pm 0.082^{+0.082}_{-0.080}$
D_s^+	$0.056 \pm 0.015 \pm 0.007$	$0.166 \pm 0.018 \pm 0.016$	$0.460 \pm 0.036 \pm 0.040$
Λ_c^+	$0.041 \pm 0.019 \pm 0.007$	$0.122 \pm 0.023 \pm 0.010$	$0.345 \pm 0.052 \pm 0.029$

Table 9: Summary of the OPAL product branching ratio measurements.

In addition we have measured the average x_E of D^0 and D^+ mesons produced from primary c quarks to be:

$$\langle x_E(\mathrm{D}^0) \rangle = 0.487 \pm 0.009^{+0.011}_{-0.009}$$

$$\langle x_E(\mathrm{D}^+) \rangle = 0.483 \pm 0.015^{+0.007}_{-0.011}$$

10.1 Measurement of $\Gamma_{c\bar{c}}/\Gamma_{had}$ by charm counting

Perhaps the most direct method of measuring $\Gamma_{c\bar{c}}/\Gamma_{had}$ is to sum the partial contributions from each of the weakly decaying charm hadrons. In addition to the states we have measured, the primary c quarks may result in strange-charmed baryons Ξ_c^+, Ξ_c^0 and Ω_c^+. Although there are no direct experimental measurements, the production rates for these baryons are expected to be much lower than that of the Λ_c^+ due to strangeness suppression. The relative rates may be estimated by reference to the light quark sector, where it is found that the Ξ^-/Λ ratio is $(6.8 \pm 0.7)\%$ and the Ω^-/Λ ratio is $(1.5 \pm 0.4)\%$ [14]. Assuming equal production of the Ξ^0 and Ξ^- states and that a similar suppression rate is applicable to the charm baryons one expects the total rate for the three strange-charmed baryons to be 15% of the Λ_c^+ rate. We refer to the scale factor necessary to convert the measured Λ_c^+ rate to the total charmed baryon rate as $S_b = 1.15$. We assign an error of ± 0.05 to this ratio when evaluating systematic errors.

To convert the measured product branching ratios given in table 9 to partial widths to the different charm states the absolute charm hadron branching ratios are required. The averages quoted by the PDG [14] for the reference modes which we use are listed in table 10.

Decay Mode	Branching fraction (%)
$D^0 \to K^-\pi^+$	3.84 ± 0.13
$D^+ \to K^-\pi^+\pi^+$	9.1 ± 0.6
$D_s^+ \to \phi\pi^+$	3.5 ± 0.4
$\Lambda_c^+ \to p^+K^-\pi^+$	4.4 ± 0.6

Table 10: PDG quoted averages for the reference branching ratios.

Particle	$\frac{\Gamma_{c\bar{c}}}{\Gamma_{had}} \cdot f(c \to X_c)\ \times 10^2$
D^0	$10.13 \pm 0.70^{+0.67}_{-0.65} \pm 0.34$
D^+	$3.93 \pm 0.50^{+0.28}_{-0.34} \pm 0.26$
D_s^+	$1.61 \pm 0.42^{+0.21}_{-0.20} \pm 0.18$
Λ_c^+ $(\times 1.15)$	$1.07 \pm 0.50^{+0.18}_{-0.19} \pm 0.21$
$\frac{\Gamma_{c\bar{c}}}{\Gamma_{had}}$	$16.7 \pm 1.1 \pm 1.1 \pm 0.5$

Table 11: Measurement of $\Gamma_{c\bar{c}}/\Gamma_{had}$ from summation of partial contributions. The errors are statistical, systematic and due to the charm branching ratios respectively. The systematic error on $\Gamma_{c\bar{c}}/\Gamma_{had}$ allows for the correlations between those on the individual measurements.

Combining our measurements with the PDG branching ratios results in the partial widths given in table 11. The total $c \to$ baryon rate is estimated by multiplying the measured $c \to \Lambda_c^+$ rate by S_b. The errors listed are statistical, systematic and external, due to uncertainties in the branching ratios, respectively. Addition of these partial widths yields:

$$\frac{\Gamma_{c\bar{c}}}{\Gamma_{had}} \quad = \quad 0.167 \pm 0.011(stat) \pm 0.011(sys) \pm 0.005(br),$$

where the combined systematic error allows for the correlations between the measurements listed in table 5. A summary of the contributions to the systematic errors is given in table 12. It is interesting to note that although the D_s^+ and Λ_c^+ branching ratios are relatively poorly known, their contribution to the total error is small because of the small partial contributions of D_s^+ and Λ_c^+ to $\Gamma_{c\bar{c}}/\Gamma_{had}$.

Source	$\Delta\left(\frac{\Gamma_{c\bar{c}}}{\Gamma_{had}}\right) \times 10^2$
INTERNAL SYSTEMATICS	
$\tau(\mathrm{B}^0)$	± 0.19
$\tau(\mathrm{B}^+)$	± 0.23
$\tau(\mathrm{B}_s^0)$	± 0.09
$\tau(\Lambda_b^0)$	± 0.07
Charm lifetimes	$^{+0.06}_{-0.07}$
b fragmentation	$^{+0.14}_{-0.19}$
c fragmentation	$^{+0.62}_{-0.67}$
f_c^{**}	± 0.08
$\Gamma_{g\to c\bar{c}}$	± 0.11
$\mathrm{d}E/\mathrm{d}x$ calibration	± 0.58
Track resolution	$^{+0.39}_{-0.36}$
Silicon matching	± 0.18
Mass fits	$^{+0.34}_{-0.36}$
Separation method	± 0.36
EXTERNAL SYSTEMATICS	
$B(\mathrm{D}^0 \to \mathrm{K}^-\pi^+)$	± 0.34
$B(\mathrm{D}^+ \to \mathrm{K}^-\pi^+\pi^+)$	± 0.26
$B(\mathrm{D}_s^+ \to \phi\pi^+)$	± 0.18
$B(\mathrm{D}_s^+ \to \overline{\mathrm{K}}^{*0}\mathrm{K}^+)/B(\mathrm{D}_s^+ \to \phi\pi^+)$	± 0.01
$B(\Lambda_c^+ \to \mathrm{pK}^-\pi^+)$	± 0.20
$S_b = 1.15 \pm 0.05$	± 0.05
TOTAL INTERNAL	± 1.1
TOTAL EXTERNAL	± 0.5

Table 12: Summary of systematic errors on the $\Gamma_{c\bar{c}}/\Gamma_{had}$ measurement from charm counting.

10.2 Comparison of primary charm hadron production rates with low energy data

It is also of interest to compare the relative production rates of the different charmed hadrons with lower energy data. The only comprehensive studies of charm production in e^+e^- annihilations are those by the CLEO [1] and ARGUS [2, 3] collaborations at $\sqrt{s} \approx 10$ GeV. These measurements are summarized in table 13.

	$\sigma \cdot B_D$ (pb)			
Experiment	D^0	D^+	D_s^+	Λ_c^+
CLEO [1]	$52 \pm 5 \pm 4$	$51 \pm 7 \pm 2$	$7.2 \pm 1.9 \pm 1.0$	$10 \pm 1.5 \pm 1.5$
ARGUS [2, 3]	43.8 ± 5.6	50.0 ± 6.9	-	$9.0 \pm 1.2 \pm 1.0$
Average	47.4 ± 4.2	50.5 ± 5.0	7.2 ± 2.1	9.4 ± 1.3

Table 13: Measured cross-sections for the reference charm decay modes at $\sqrt{s} \approx 10$ GeV.

In order to calculate the fraction of primary c quarks which result in each of the weakly decaying species we have used the PDG charm branching ratios listed in table 10. For both the OPAL and low energy results the total charm production rate was assumed to be saturated by the three charm mesons plus the measured Λ_c^+ rate, scaled by $S_b = 1.15 \pm 0.05$ to allow for the strange-charmed baryons. The charm fractions listed in table 14 were then calculated from the ratios of the separate contributions to the total rates.

Particle	OPAL (%)	CLEO/ARGUS (%)
D^0	60.5 ± 3.7 (± 1.5)	55.1 ± 3.1 (± 1.6)
D^+	23.5 ± 2.9 (± 1.3)	24.7 ± 2.3 (± 1.4)
D_s^+	9.6 ± 2.5 (± 1.0)	9.2 ± 2.5 (± 1.0)
Λ_c^+	5.6 ± 2.5 (± 0.8)	9.5 ± 1.3 (± 1.3)

Table 14: Comparison of the results of the fit to our measurements of charm production rates from primary c quarks with the average of the CLEO and ARGUS measurements. The errors in parentheses are due to the common uncertainties in the charmed hadron branching ratios.

Comparing the results shows that there is good agreement between the two energies on the relative production rates of the different charmed hadron species.

10.3 Measurement of the charm hadron multiplicity in *b* decays

Because of the dominance of the $b \to c$ weak transition nearly all $\overline{\mathrm{B}}$ meson or b baryon decays are expected to result in a hadron containing a c quark. In addition $\bar{c}$ quarks may result from virtual $\mathrm{W}^- \to \bar{c}s$ process in the decay. Experimentally it is easier to measure the total yield of c and $\bar{c}$ quarks, n_c. To a good approximation this should be equal to $1 + B(b \to c\bar{c}s)$. Theoretical estimates for n_c are typically in the range 1.11 to 1.30 [6, 7]. The estimates depend strongly on the assumed b and c quark masses. However, because these also enter into the calculation of the semileptonic decay widths, which are experimentally well determined [14], a comparison of the two provides a significant test of the theory. Recently it has been suggested that a value of $n_c = 1.28 \pm 0.08$ is required [7] to make the theory consistent with the measured semileptonic branching ratios.

The ARGUS [2, 4] and CLEO [5] experiments have measured the production of charmed hadrons in B^+ and B^0 meson decays produced at the $\Upsilon(4S)$. These measurements favour values of n_c at the lower end of the theoretical expectations. A recent review of the $\Upsilon(4S)$ results [27] obtains $n_c = 1.10 \pm 0.06$. It is therefore of significant interest to measure n_c for b hadrons produced in Z^0 decays, where the mix of b hadrons and experimental systematics are different. In order to study n_c we have divided our measurements listed in table 9 by $\Gamma_{b\bar{b}}/\Gamma_{had} = 0.2216 \pm 0.0017$ [28] and the appropriate charm branching ratios. The results are listed in table 15. The sum of the four charmed hadrons is found to account for:

$$1.061 \pm 0.045 \pm 0.060 \pm 0.037$$

c or $\bar{c}$ quarks per b-hadron decay, where the errors are statistical, systematic and external, due to the charm branching ratios, respectively. The systematic error allows for the correlations between the errors on the individual measurements and includes a small contribution from the uncertainty on $\Gamma_{b\bar{b}}/\Gamma_{had}$.

The only other states which may contribute to n_c are the strange charmed baryons and charmonium mesons. We make no attempt to correct for the strange charmed baryons; however, due to strangeness suppression these are not expected to give a large contribution to n_c. The total rate to charmonium states may be estimated from the OPAL measurement of the $B(b \to \mathrm{J}/\psi\mathrm{X}) = (1.15 \pm 0.06 \pm 0.12)\%$ rate [29]. Assuming the relative production rates of the different charmonium states is $1 : 0.57 : 0.27 : 0.31$ for the $\mathrm{J}/\psi : \eta_c : \chi_{c1} : \psi'$ as predicted in reference [30] and allowing for feed-down a correction scale factor of 1.7 is estimated. This must be further multiplied by 2, to allow for the c and $\bar{c}$ quark in the charmonium states. Applying this correction to the the OPAL measurement we estimate a contribution of $0.039 \pm 0.002 \pm 0.004$ to n_c. Here no errors have been added due to the uncertainties in the correction factor. Since the total charmonium rate is small, and dominated by direct and indirect J/ψ production, it is not a significant contribution to the overall uncertainty. With the addition of the charmonium contribution, the measured states are found to correspond to a charm quark multiplicity of

$$1.100 \pm 0.045 \pm 0.060 \pm 0.037$$

c or $\bar{c}$ quarks per b hadron decay.

In table 15 we compare our results with a recent review of $\Upsilon(4S)$ measurements [27]. To facilitate comparison the averages given in [27] have been adjusted to use the charm hadron branching ratios listed in table 10. It should be noted the $\Upsilon(4S)$ averages include some preliminary results. The comparison indicates that, as expected, the relative production rates

Particle	OPAL (%)	$\Upsilon(4S)$ (%)
D^0	$53.4 \pm 2.7 \pm 3.1(\pm 1.8)$	$63.1 \pm 2.0(\pm 2.1)$
D^+	$18.8 \pm 1.5 \pm 1.3(\pm 1.2)$	$24.2 \pm 3.1(\pm 1.6)$
D_s^+	$21.4 \pm 2.3 \pm 2.1(\pm 2.5)$	$10.4 \pm 0.9(\pm 1.2)$
Λ_c^+	$12.5 \pm 2.4 \pm 1.0(\pm 1.7)$	$4.6 \pm 0.7(\pm 0.6)$
Ξ_c^+ and Ξ_c^0	-	3.9 ± 1.5
Sum of charmed hadrons	$106.1 \pm 4.5 \pm 6.0(\pm 3.7)$	$106.2 \pm 4.1(\pm 3.0)$
charmonia ($\times 2$)	$3.9 \pm 0.2 \pm 0.4$	3.6 ± 0.3
Total	$110.0 \pm 4.5 \pm 6.0(\pm 3.7)$	$109.8 \pm 4.2(\pm 3.0)$

Table 15: Comparison of our results on charm production rates in b hadron decays with $\Upsilon(4S)$ measurements. The errors in parenthesis are due to the uncertainties in the charm branching ratios and are common between the measurements.

of D_s^+ and Λ_c^+ hadrons are larger in our data and that there is a corresponding reduction in the rates of D^0 and D^+ mesons. Despite the different mixture of charm hadrons, the total charm multiplicity is in good agreement with the $\Upsilon(4S)$ measurements. All of the charm multiplicity measurements rely on the absolute charm hadron branching ratios and because those of the D_s^+ and Λ_c^+ hadrons are relatively poorly determined, there is a possibility that the values quoted in [14] are inaccurate. However, because our data and the $\Upsilon(4S)$ measurements have different sensitivity to the D_s^+ and Λ_c^+ branching ratios, the good agreement observed disfavours significant inaccuracies in these branching ratios.

11 Summary and Conclusions

Using 1.71 million hadronic Z^0 decays we have studied the production of D^0, D^+, D_s^+ and Λ_c^+ hadrons. Using the PDG average charm branching ratios, the overall production rates are found to correspond to multiplicities of

$$\begin{aligned} 0.465 \pm 0.017 \pm 0.022 \pm 0.016 \quad & D^0, \\ 0.170 \pm 0.009 \pm 0.009 \pm 0.011 \quad & D^+, \\ 0.131 \pm 0.010 \pm 0.011 \pm 0.014 \quad & D_s^+, \\ 0.078 \pm 0.012 \pm 0.006 \pm 0.010 \quad & \Lambda_c^+ \end{aligned}$$

hadrons per hadronic Z^0 decay. The errors are statistical, systematic and due to the charm branching ratios respectively. Using decay length information we have separated the contributions from b hadron decays and prompt production.

The measurements of the rates of charm hadrons formed from primary c quarks have been used to measure $\Gamma_{c\bar{c}}/\Gamma_{had}$. By summing the partial contributions from D^0, D^+, D_s^+ and Λ_c^+ and estimating the small contribution from strange-charmed baryons, we have made a direct measurement of

$$\frac{\Gamma_{c\bar{c}}}{\Gamma_{had}} = 0.167 \pm 0.011(stat) \pm 0.011(sys) \pm 0.005(br),$$

where the errors are statistical, systematic and due the uncertainties in the charm hadron branching ratios, respectively. This result is in good agreement with the Standard Model prediction of 0.172 [26] and with other LEP results [24, 31]. Unlike some other methods this technique is not severely limited by external systematic errors and there is considerable scope for improvements as more data are analysed.

Comparison of our results on the relative production rates of the different charmed hadron species from primary c quarks shows good agreement with ARGUS and CLEO data. The composition of the hadrons arising from primary charm quarks is currently one of the largest systematic errors in measurements of $\Gamma_{b\bar{b}}/\Gamma_{had}$ and our results should lead to a significant reduction in this.

Combining our measurements of D^0, D^+, D_s^+ and Λ_c^+ production in b hadron decays, we find that these states account for

$$1.061 \pm 0.045(stat) \pm 0.060(sys) \pm 0.037(br)$$

c or $\bar{c}$ quarks per b hadron decay. The addition of the contribution from charmonium states which is estimated from OPAL data increases this to $1.100 \pm 0.045(stat) \pm 0.060(sys) \pm 0.037(br)$. Since the contribution from strange-charmed baryons is expected to be small, our measurements confirm the observation of ARGUS and CLEO that n_c is at the lower end of theoretical expectations. In particular it would be difficult to accommodate the prediction of $n_c = 1.28 \pm 0.08$ [7] with the data. Since this implies a higher theoretical prediction for the semileptonic widths of b hadrons, it makes these measurements more difficult to understand.

Acknowledgements

It is a pleasure to thank the SL Division for the efficient operation of the LEP accelerator and for their continuing close cooperation with our experimental group. In addition to the support staff at our own institutions we are pleased to acknowledge the
Department of Energy, USA,
National Science Foundation, USA,
Particle Physics and Astronomy Research Council, UK,
Natural Sciences and Engineering Research Council, Canada,
Israel Ministry of Science,
Israel Science Foundation, administered by the Israel Academy of Science and Humanities,
Minerva Gesellschaft,
Japanese Ministry of Education, Science and Culture (the Monbusho) and a grant under the Monbusho International Science Research Program,
German Israeli Bi-national Science Foundation (GIF),
Direction des Sciences de la Matière du Commissariat à l'Energie Atomique, France,
Bundesministerium für Bildung, Wissenschaft, Forschung und Technologie, Germany,
National Research Council of Canada,
Hungarian Foundation for Scientific Research, OTKA T-016660, and OTKA F-015089.

References

[1] CLEO Collaboration, D. Bortoletto *et al.*, *Phys. Rev.* **D37** (1988) 1719; *Erratum Phys. Rev* **D39** (1989) 1471;
CLEO Collaboration, P. Avery *et al.*, *Phys. Rev.* **D43** (1991) 3599.

[2] ARGUS Collaboration, H. Albrecht *et al.*, *Z. Phys.* **C52** (1991) 353.

[3] ARGUS Collaboration, H. Albrecht *et al.*, *Phys. Lett.* **B207** (1988) 109.

[4] ARGUS Collaboration, H. Albrecht *et al.*, *Phys. Lett.* **B210** (1988) 263;
ARGUS Collaboration, H. Albrecht *et al.*, *Z. Phys.* **C54** (1992) 1.

[5] CLEO Collaboration, D. Bortoletto *et al.*, *Phys. Rev.* **D45** (1992) 21;
CLEO Collaboration, G. Crawford *et al.*, *Phys. Rev.* **D45** (1992) 752.

[6] See for example: G. Altarelli and S. Petrarca, *Phys. Lett.* **B261** (1991) 303.

[7] E. Bagan, P. Ball, V.M. Braun and P. Gosdzinsky, *Nucl. Phys.* **B432**, (1994) 3.

[8] OPAL Collaboration, K. Ahmet *et al.*, *Nucl. Instr. Meth.* **A305** (1991) 275;
P. P. Allport *et al.*, *Nucl. Instr. Meth.* **A324** (1993) 34;
P. P. Allport *et al.*, *Nucl. Instr. Meth.* **A346** (1994) 476.

[9] M. Hauschild *et al.*, *Nucl. Instr. Meth.* **A314** (1992) 74.

[10] OPAL Collaboration, G. Alexander *et al.*, *Z. Phys.* **C52** (1991) 175.

[11] C. Peterson, D. Schlatter, I. Schmitt and P. M. Zerwas, *Phys. Rev.* **D27** (1983) 105.

[12] T. Sjöstrand, Comp. Phys. Comm. **39** (1986) 347;
M. Bengtsson and T. Sjöstrand, Comp. Phys. Comm. **43** (1987) 367.

[13] OPAL Collaboration, G. Alexander *et al.*, *Z. Phys.* **C69** (1996) 543.

[14] Particle Data Group, L. Montanet *et al.*, *Phys. Rev. Lett.* **D50** (1994) 1173.
The $D^0 \to K^-\pi^+$ branching ratio has been updated to correspond to the preliminary 1996 averages.

[15] ALEPH Collaboration, D. Buskulic *et al.*, *Z. Phys.* **C62** (1994) l.

[16] DELPHI Collaboration, P. Abreu *et al.*, *Phys. Lett.* **B345** (1995) 598;
OPAL Collaboration, R. Akers *et al.*, *Z. Phys.* **C66** (1995) 19;
ALEPH Collaboration, D. Buskulic *et al.*, *Z. Phys.* **C69** (1996) 393.

[17] OPAL Collaboration, R. Akers *et al.*, *Z. Phys.* **C67** (1995) 379;
OPAL Collaboration, R. Akers *et al.*, *Phys. Lett.* **B350** (1995) 273;
OPAL Collaboration, R. Akers *et al.*, *Phys. Lett.* **B353** (1995) 402;
OPAL Collaboration, R. Akers *et al.*, *Z. Phys.* **C69** (1996) 195;
ALEPH Collaboration, D. Buskulic *et al.*, *Z. Phys.* **C69** (1996) 585;
ALEPH Collaboration, D. Buskulic *et al.*, *Phys. Lett.* **B357** (1995) 685;
DELPHI Collaboration, P. Abreu *et al.*, *Z. Phys.* **C68** (1995) 375;

DELPHI Collaboration, P. Abreu *et al.*, *CERN-PPE/95-059* (1995);
DELPHI Collaboration, P. Abreu *et al.*, *Z. Phys.* **C68** (1995) 13;
CDF Collaboration, F. Abe *et al.*, *Phys. Rev. Lett.* **72** (1994) 3456;
CDF Collaboration, F. Abe *et al.*, *Phys. Rev. Lett.* **74** (1995) 4988.

[18] OPAL Collaboration, G. Alexander *et al.*, *Phys. Lett.* **B364** (1995) 93.

[19] J. Allison *et al.*, *Nucl. Instr. Meth.* **A317** (1992) 47.

[20] P. Collins and T. Spiller, *J. Phys.* **G11** (1985) 1289.

[21] V. G. Kartvelishvili, A. K. Likhoded and V. A. Petrov, *Phys. Lett.* **B78** (1978) 615.

[22] B. Anderson, G. Gustafson and B. Söderberg, *Z. Phys.* **C20** (1983) 317.

[23] OPAL Collaboration, R. Akers *et al.*, *Z. Phys.* **C67** (1995) 27.

[24] OPAL Collaboration, R. Akers *et al.*, *Phys. Lett.* **B353** (1995) 595.

[25] OPAL Collaboration, M. Z. Akrawy *et al.*, *Z. Phys.* **C47** (1990) 505.

[26] Calculated using the ZFITTER program assuming $M_{Higgs} = 300$ GeV and $M_{top} = 180$ GeV.
D. Bardin *et al.*, *Z. Phys.* **C44** (1989) 493;
D. Bardin *et al.*, *Nucl. Phys.* **B351** (1991) 290;
D. Bardin *et al.*, *Phys. Lett.* **B255** (1991) 493.

[27] T. E. Browder and K. Honscheid, *Prog. in Nucl. and Part. Phys.* **35** (1995).

[28] The LEP Collaborations and the LEP Electroweak Working Group, *CERN-PPE/95-172* (1995).

[29] OPAL Collaboration, G. Alexander *et al.*, *CERN-PPE/95-153* (1995), to appear in *Z. Phys.* **C**.

[30] J. H. Kühn, S. Nussinov and R. Rückl, *Z. Phys.* **C5** (1980) 117.

[31] ALEPH Collaboration, D. Buskulic *et al.*, *Phys. Lett.* **B244** (1990) 551;
DELPHI Collaboration, P. Abreu *et al.*, *Phys. Lett.* **B252** (1990) 140;
DELPHI Collaboration, P. Abreu *et al.*, *Phys. Lett.* **B295** (1992) 383;
DELPHI Collaboration, P. Abreu *et al.*, *Z. Phys.* **C59** (1993) 533.

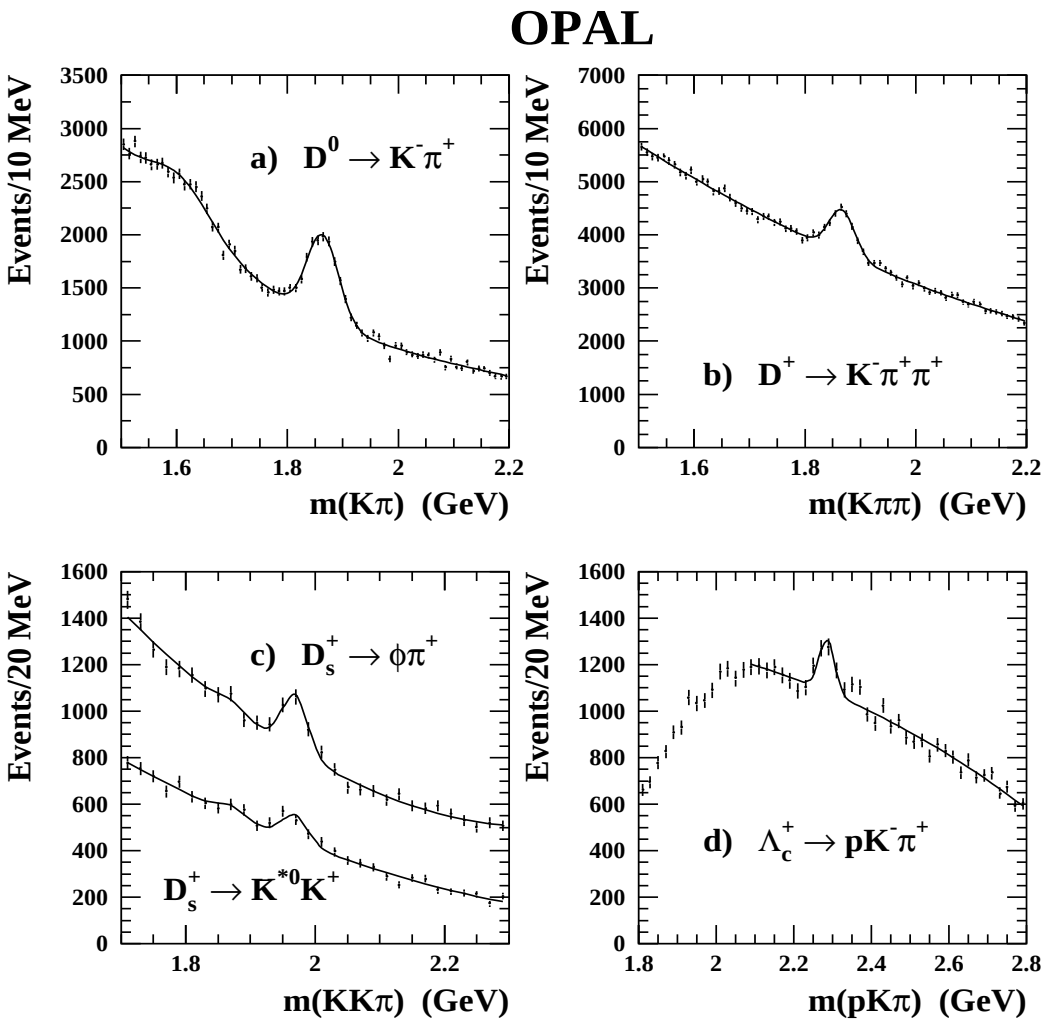

Figure 1: Mass distributions for a) $K^-\pi^+$, b) $K^-\pi^+\pi^+$, c) $K^-K^+\pi^+$ and d) $pK^-\pi^+$ combinations. In each case the points are the data and the curves are the fits.

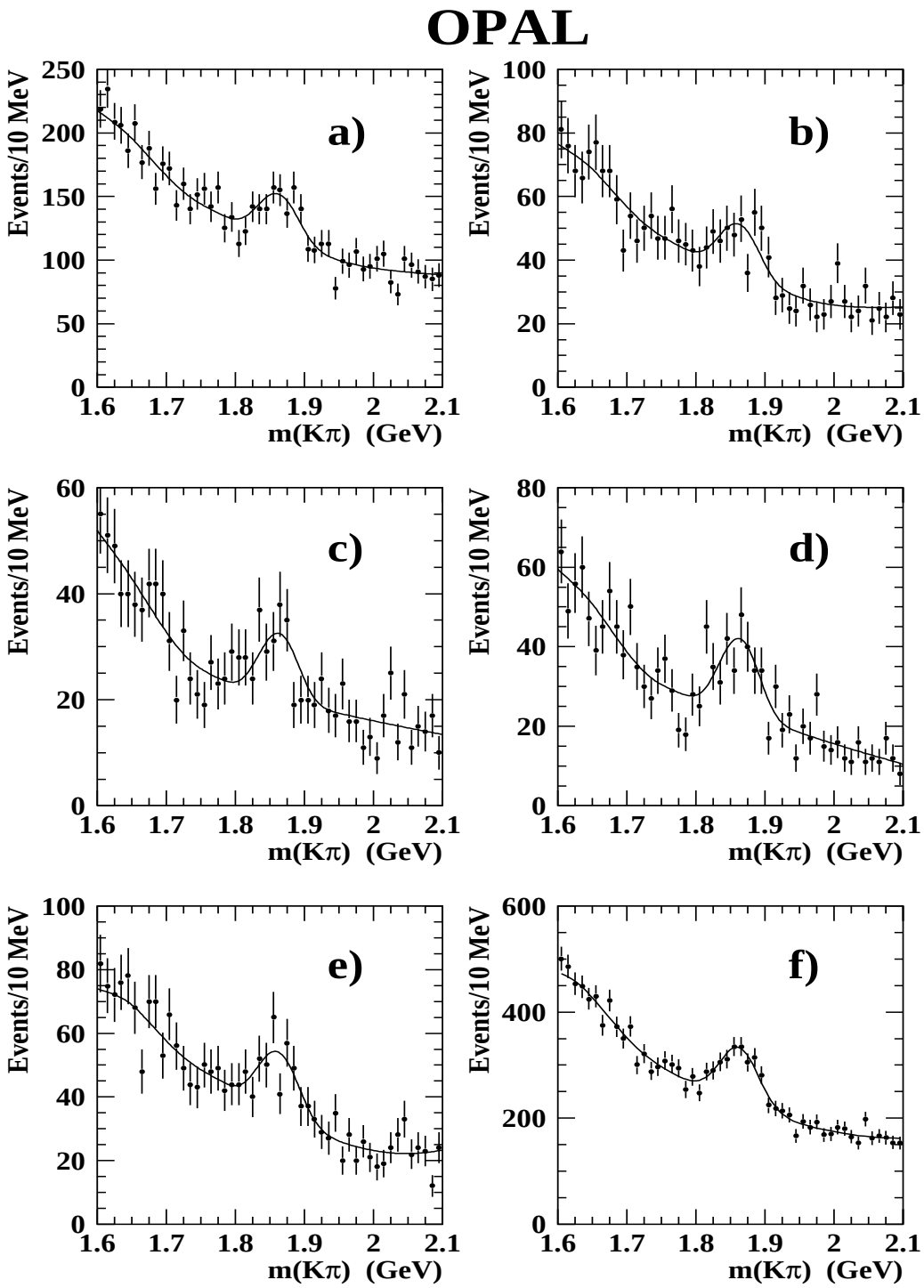

Figure 2: Results of the mass fit for the $D^0 \to K^-\pi^+$ data in the x_E region 0.20-0.25 divided into the five decay length regions a) 0.05-0.15 cm, b) 0.15-0.25 cm, c) 0.25-0.35 cm, d) 0.35-0.55 cm, e) 0.55-2.00 cm and f) the total. In each case the points are the data and the histogram is the result of the maximum likelihood fit.

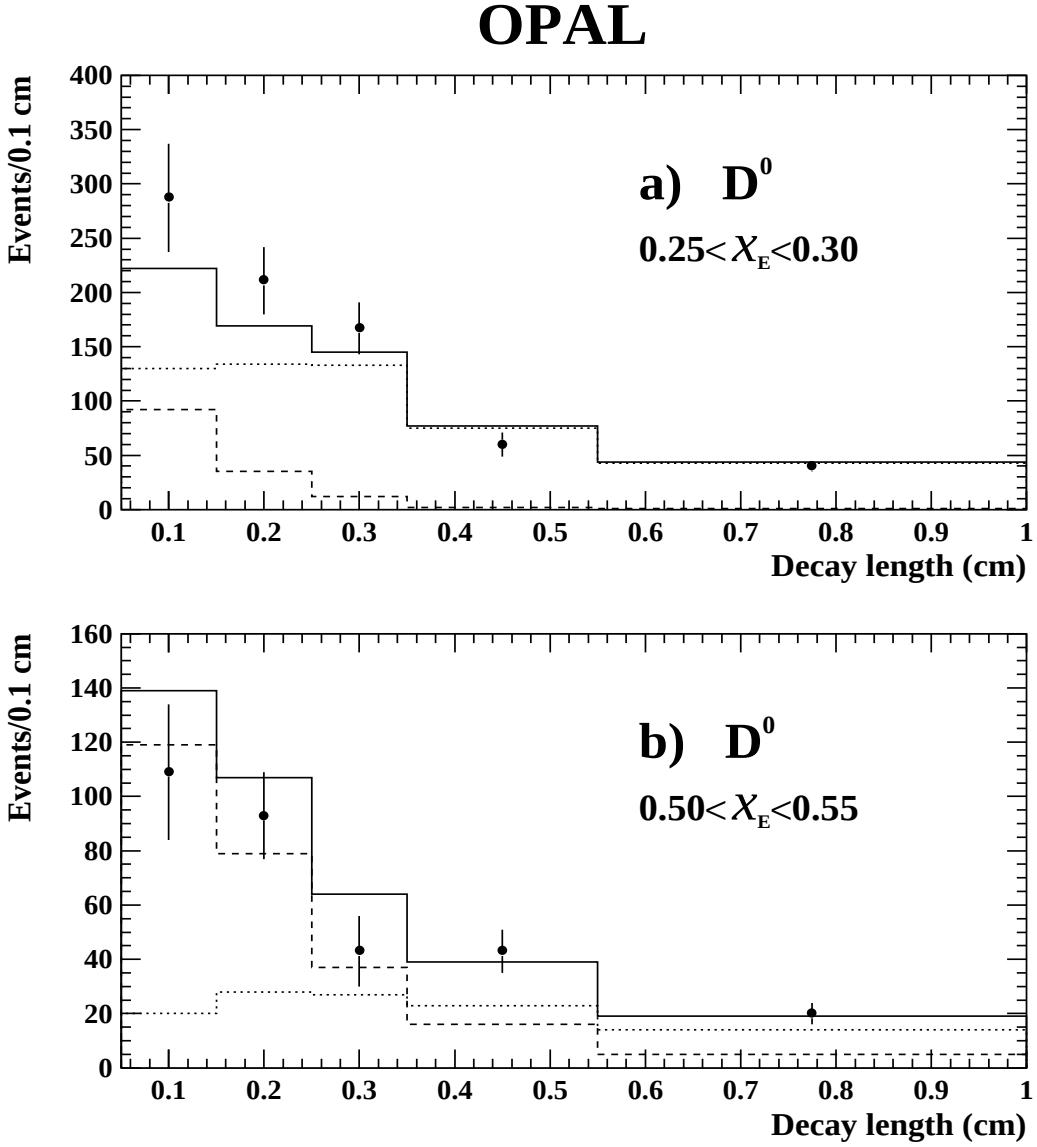

Figure 3: Results of the Peterson fragmentation fit for two of the 13 different x_E regions of the $D^0 \to K^-\pi^+$ data. a) $0.25 < x_E < 0.30$ and b) $0.50 < x_E < 0.55$. In both cases the points are the data and the solid histograms are the results of the simultaneous fit to all the x_E regions. The dashed and dotted histograms show the contributions from the prompt and $b \to D^0$ components, respectively.

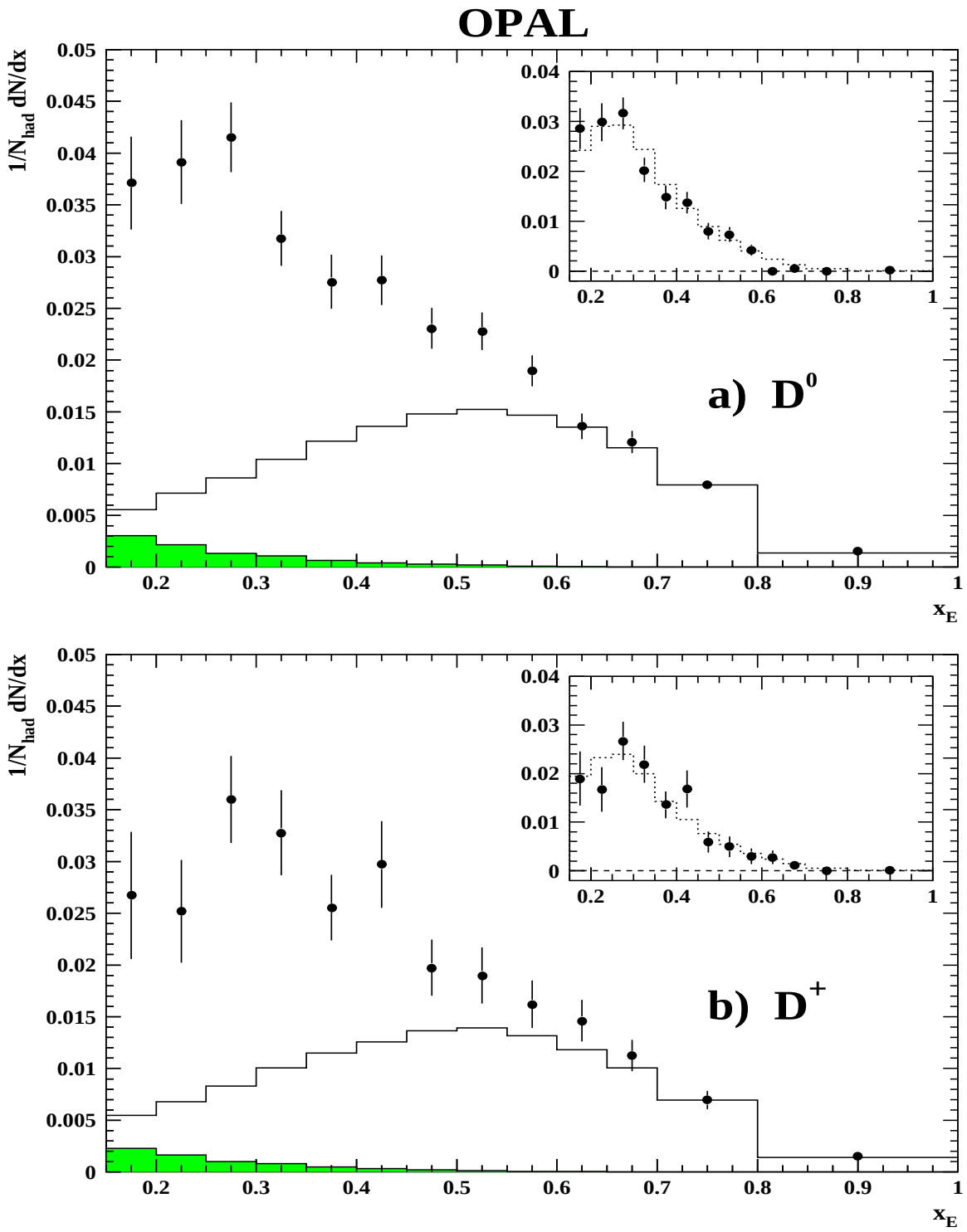

Figure 4: Results of the source separation fits assuming Peterson fragmentation for $Z^0 \to c\bar{c}$ decays: a) D^0 and b) D^+. In the main plots the histograms indicate the fitted $c \to D$ component, the solid region is the fixed contribution from $g \to DX$ and the points are the total including $b \to D$. In the inserts the unfolded energy spectra for $b \to D$ decays are compared with the predictions of the JETSET simulation.

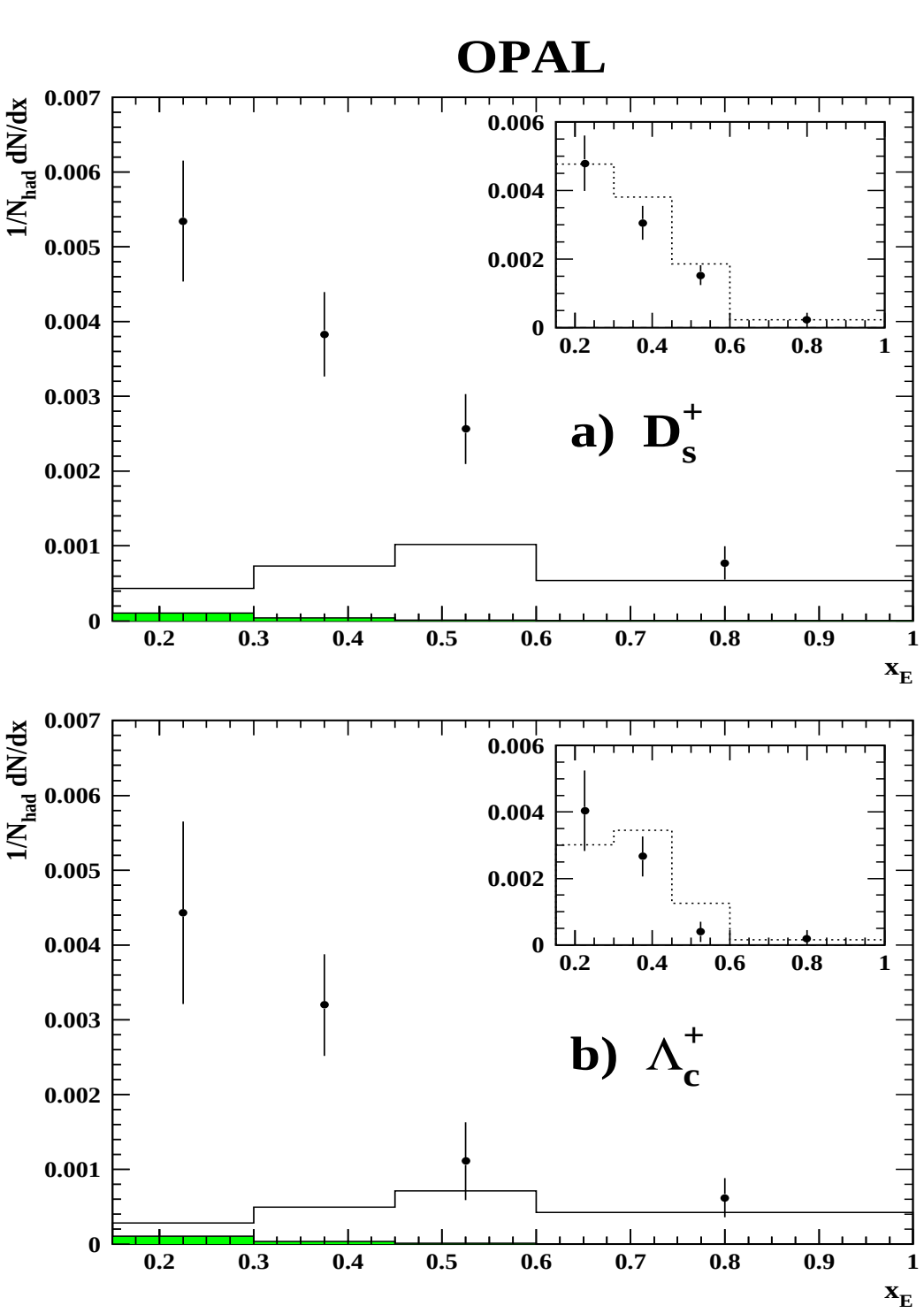

Figure 5: Results of the source separation fits assuming Peterson fragmentation for $Z^0 \to c\bar{c}$ decays: a) D_s^+ and b) Λ_c^+. In each case the histogram indicates the fitted $c \to X_c$ component, the solid region is the fixed contribution from gluon splitting and the points are the total including $b \to X_c$. In the inserts the unfolded energy spectra for $b \to X_c$ decays are compared with the predictions of the JETSET simulation.